Dear Editor,

Please find enclosed our revised manuscript. We have addressed the reviewers' comments as outlined in the responses to the reviewers uploaded earlier. In some cases, restructuring of the manuscript and changes in results have meant that our text changes deviate somewhat from our earlier response (all changes are highlighted in the marked-up manuscript version).

Overall, we have restructured the paper and collected all methodical descriptions that had previously been scattered across sections 2, 3, and 4, now in one place in section 2. We have clarified the methods to better explain the differences between the three emulator approaches.

In the first submission, the emulators had been trained using only data from RCP8.5. After adding the significance test as suggested by the reviewers, and doing some more testing, we have decided to use all available data from all four RCPs to train the emulator. This has improved overall emulator performance and has led to extensive changes to the results in section 3.2 and 4. Results for the emulators trained only on RCP8.5 are still available in the Supplement, and the effect of using either the full or limited training data is discussed at several points in sections 3.2 and 4.

Moreover, we discovered that pDSSAT (one of the crop models) deviated from the simulation protocol which meant that we had to redo the analysis for this model. We have added descriptions of the differences between model settings of pDSSAT and the other models in section 2 and added text to the results sections where these differences in simulation setup lead to differences in the results.

Attached to this letter you will find a marked-up manuscript version showing all changes to the text. In addition to the text changes, we have also updated all figures. Figure updates include better colour scales, increased font sizes for the labels, and improved figure layouts to make better use of the available space.

We believe that the manuscript has improved substantially thanks to the reviews, and hope that it is now acceptable for publication in ESD. We look forward to your response, and remain at your disposal for any further questions.

For the authors,

Sebastian Ostberg, Jacob Schewe

Changes in crop yields and their variability at different levels of global warming

Sebastian Ostberg[1,2], **Jacob Schewe**[1], **Katelin Childers**[1], **and Katja Frieler**[1]

[1]Potsdam Institute for Climate Impact Research, Telegrafenberg A31, 14473 Potsdam, Germany
[2]Geography Department, Humboldt-Universität zu Berlin, Berlin, Germany

Correspondence: Sebastian Ostberg (ostberg@pik-potsdam.de)

Abstract. An assessment of climate change impacts at different levels of global warming is crucial to inform the political discussion about mitigation targets, as well as for the economic evaluation of climate change impacts e.g. in economic models such as Integrated Assessment Models (IAMs) that internally that only use global mean temperature change as indicator of climate change. There is already a well-established framework for the scalability of regional temperature and precipitation changes with global mean temperature change (ΔGMT). It is less clear to what extent more complex, biological or physiological impacts such as crop yield changes can also be described in terms of ΔGMT; even though such impacts may often be more directly relevant for human livelihoods than changes in the physical climate. Here we show that crop yield projections can indeed be described in terms of ΔGMT to a large extent, allowing for a fast interpolationestimation of crop yield changes tofor emission scenarios not originally covered by climate and crop model projections. We use an ensemble of global gridded crop model simulations for the four major staple crops to show that the scenario dependence is a minor component of the overall variance of projected yield changes at different levels of ΔGMT. In contrast, the variance is dominated by the spread across crop models. Varying CO_2 concentrations are shown to explain only a minor component of the remaining crop yield variability at different levels of global warming. In addition, we show that the variability of crop yields is expected to increase with increasing warming in many world regions. We provide, for each crop modeland climate model, patterns of mean yield changes that allow for a simplified description of yield changes under arbitrary pathways of global mean temperature and CO_2 changes, without the need for additional climate and crop model simulations.

1 Introduction

Climate change exerts a substantial and direct impact on food security and hunger risk by altering the global patterns of precipitation and temperature which determine the location of arable land (Parry et al., 2005; Rosenzweig et al., 2014) as well as the quality (Müller et al., 2014) and quantity (Müller and Robertson, 2014; Lobell et al., 2012; van der Velde et al., 2012) of crops comprising most of the world food supply. Climate change alone By itself, climate change is expected to reduce global production of the four major crops wheat, maize, soy and rice on current agricultural areas (e.g., Rosenzweig et al., 2014; Challinor and Wheeler, 2008; Peng et al., 2004). Facing an increasing food demand due to population growth and economic development, these reductions will have to be overcompensated compensated by 1) the direct physiological impacts of increased atmospheric CO_2 concentrations (Kimball, 1983), which are beyond local human control; as well as 2) advances in agricultural management (e.g. fertilizer input or irrigation), technology, and breeding (Jaggard et al., 2010) or 3) expansion of agricultural land (Frieler et al., 2015; Smith et al., 2010).

In conjunction with these long term changes, global warming is also expected to contribute to an increase in the frequency and duration of extreme temperatures and precipitation (droughts, floods, and heat waves), which may increase the near term variability of crop yields and trigger short term crop price fluctuations (Brown and Kshirsagar, 2015; Mendelsohn et al., 2007; Tadesse et al., 2014).

The emission Anthropogenic emissions of greenhouse gases is are expected to influence crop yields via several channelspathways. On the one hand, the associated climate cli-

matic changes will modify the length of the growing season (Eyshi Rezaei et al., 2014), water availability, and heat stress (Lobell et al., 2012; Müller and Robertson, 2014; Schlenker and Roberts, 2009); and on the other hand, higher concentrations of atmospheric CO_2 are expected to increase the water use efficiency in C3 (e.g. wheat, rice, soy) and C4 (maize) crops, and enhance the rate of photosynthesis in C3 crops (Darwin and Kennedy, 2000). Global Gridded Crop Models (GGCMs) are particularly designed to account for these effects. They provide a complex process-based implementation of our current understanding of the mechanisms underlying crop growth, and are the primary tool for crop yield projections (e.g., Rosenzweig et al., 2014) which in turn are a prerequisite for assessing potential changes in prices (Nelson et al., 2014) and food security (Parry et al., 2005).

However, these process-based crop yield projections rely on spatially explicit realizations of the driving weather variables such as temperature, precipitation, radiation, and humidity, often at daily resolution, as provided by computationally expensive Global Climate Model (GCM) simulations. The GGCMs themselves also require significant computational capacity. These requirements generally limit the number and duration of emission scenarios that can be considered.

The so-called pattern scaling approach is a well-established method to overcome these limits. Output from GCMs has been shown to be, to some extent, scalable to different global mean temperature (GMT) trajectories not originally covered by GCM simulations (Santer et al., 1990; IPCC-TGICA, 2007; Mitchell, 2003; Giorgi, 2008; Solomon et al., 2009; Frieler et al., 2012; Heinke et al., 2013)(Santer et al., 1990; Mitchell, 2003; IPCC-TGICA, 2007; Giorgi, 2008; Solomon et al., 2009; Frieler et al., 2012; Heinke et al., 2013). Scaled climate projections have also been used as input for different impact models (Ostberg et al., 2013; Stehfest et al., 2014) to gain flexibility with regard to the range of emission scenarios considered.

Building upon such a framework, we present a method to extend the capacity of crop yield impact projections by relating simulated crop yields yield changes to two highly aggregated quantities – global mean temperature change (ΔGMT) and atmospheric CO_2 concentration (pCO_2) – by means of simplified function. ΔGMT and pCO_2 are the standard output standard outputs of simple climate models, which allow for highly efficient climate projections for any emissions scenario by emulating the response of the complex GCMs (Meinshausen et al., 2011). Here "emulating" means that the simplified representation is designed to reproduce the complex model response response of the complex model for the originally simulated scenarios but also allows for its inter- or extrapolation to other scenarios. In this way our We test to what extent crop yield changes, as one example of climate change impacts, can be described directly in terms of GMT and pCO_2 changes. Our approach is different from other emulators building on regional which use spatially explicit climate projections as input for the simplified functions emulating complex crop models' responses to these forcings (Blanc, 2017)(Oyebamiji et al., 2015; Blanc, 2017). While these approaches only emulate the crop model responsesresponses of the complex crop model, the approach presented here implicitly provides a simplified description of both the GCMs' regional patterns of climate change and the associated response of the crop models.

We test to what extent climate change impacts such as crop yields can be directly described in terms of GMT (and pCO_2) changes without an intermediate scaling of the regional climate changes. Such a direct description of the simulated impacts – in contrast to scaling the climate changes for specific emission scenarios and then using the scaled climate projections as input for impact model simulations – has the advantage of saving computation timeprovides high computational efficiency, making the approach e.g. applicablewithin applicable, for example, in Integrated Assessment Modelsand even when no impact model is accessible. In principle, scaled but spatially explicit climate projections could also be used as input for spatial explicit crop model emulators (Blanc, 2017) to reach high efficiency. However, in this case the scaling of other emulators could be used in this setting, however requiring an additional step of first scaling the climate changes to the climate information has to be carefully adjusted to provide the kind of climate information required by the impact model impact emulator and this two-step approach also mean two approximations that may lead to higher deviations than the one-step approach proposed herespecific emission scenario.

The emulator introduced here allows for multi-impact-model multi-crop-model projections for arbitrary emission scenarios as long as crop-model ensemble projections are available for a limited set of scenarios. This offers a practical way of keeping track of a relevant but often-ignored source of uncertainty which is manifested in the considerable spread across different crop models and other process-based impact models (Rosenzweig et al., 2014; Schewe et al., 2014). This uncertainty is particularly critical when estimating socio-economic consequences (e.g., Nelson et al., 2014).

We test the approach using an ensemble of yield projections of the four major cereal crops (crops maize, rice, soy, and wheat), generated within the first phase ("Fast Track") of the Inter-sectoral Impact Model Intercomparison Project (ISIMIP, Warszawski et al., 2014). For a number of ΔGMT intervals we compare the spread in yield outcomes induced by the choice of emission scenario with that induced by the choice of GGCM and GCM, respectively. A low scenario-induced spread means that GCM- and GGCM-specific yield projections can be approximated by a simplified relationship with global mean temperature change without accounting for the underlying emission scenario, which is a prerequisite to applying the simplified relationship to other emission scenarios. The test is done at each grid cell point and separately for simulations of purely rain-fed yields and fully irrigated yields. Multi-model ensembles of crop yields over such a wide range of crops, CO_2 concentrations, and irrigation options are a new prospect and the ISIMIP data provides a uniquely broad suite of crop yield impact simulations encompassing output from five GGCMs, forced with output from up to five GCMs, and four Representative Concentration Pathways (RCPs, van Vuuren et al., 2011).

In Section 2 we describe the ISIMIP data and the methods used to test for scenario dependence and adjustment for different levels of copCO$_2$. Section 3 is dedicated to the presentation of the projected average changes in crop yields at different levels of global warming and an attribution of the variance of these long term changes to different sources of uncertainty, i.e., different GCMs, different GGCMs, and different emission scenarios (subsection 3.1). The simulated impacts of climate and CO2 changes on global and regional crop yields are shown to be related to global mean temperature change, and to be largely independent of the emissions scenario. In addition, we test to what degree the scenario-dependence of crop yields at different levels a specific level of global warming can be explained by different levels of copCO$_2$ (subsection 3.2). Thus, finally Finally, we provide individual maps of yield changes at different levels of global mean temperature GMT and the additional effect of variations in copCO$_2$ concentration at given global mean temperature at the respective GMT levels. We propose three methods to generate these patterns based on the available complex model simulations, and describe the related approaches to estimate GGCM- and GCM-specific yield changes for new ΔGMT trajectories not originally covered by GCM-crop-model simulations. In Section 4 we present a quantification of the projection errors as compared to actual simulations by the complex gridded crop modelmodels. Finally, in Section 5 we quantify the residual inter-annualvariance of the simulated crop yields in terms of global mean temperature change for each combination GMT change across all combinations of crop and climate models. Section 6 provides a summary.

2 Data and Methods

2.1 Crop yield simulations

We use projections from five different GGCMs (GEPIC, LPJ-GUESS, LPJmL, PEGASUS, and pDSSAT) that participated in in the first simulations the first simulation round of ISIMIP (Rosenzweig et al., 2014; Warszawski et al., 2014) in order to test for a dependence of projected yield changes on the global mean temperature GMT pathway (see Table 1 for their basic characteristics). Each crop model was forced by climate projections of from five different GCMs (HadGEM2-ES, IPSL-CM5A-LR, MIROC-ESM-CHEM, GFDL-ESM2M, NorESM1-M) generated for four RCPs (RCP2.6, RCP4.5, RCP6.0, RCP8.5) in the context of the Coupled Model Intercomparison Project, phase 5 ((CMIP5, Taylor et al., 2012). CMIP5 was an effort by the climate modelling community to provide a new suite of climate simulations in time for the Intergovernmental Panel on Climate Change (IPCC) Fifth Assessment Report (AR5). The RCPs cover the range from climate mitigation (RCP2.6, RCP4.5) to business-as-usual (RCP6.0) and high emissions scenarios (RCP8.5). Climate projections have been bias-corrected to better match observed historical averages of the considered climate variables. For the future, the bias-correction preserves absolute changes in monthly temperature and relative changes in monthly values of the other variables simulated by the GCMs while also correcting the daily variability about the monthly mean (Hempel et al., 2013). Separate simulations are available for each of the four major crops: wheat, maize, rice and soy, on a global 0.5 x 0.5 degree grid, covering the time period from 1971–2099. The considered crop is assumed to grow everywhere on the global land area, only restricted by soil characteristics and climate but independent of present or future land use patterns ("pure crop" simulations). Each model has provided a pair of simulations ("runs") for each climate change scenario: 1) a rain-fed run and 2) a full-irrigation run assuming no water constraints. This design provides full flexibility with regard to the application of future land use and irrigation patterns. While the "default" crop yield simulations ($Y_{\mathrm{CO2}}Y_{\mathrm{varCO2}}$) account for the fertilization effects due to the increasing levels of atmospheric copCO$_2$, the ISIMIP setting also includes a sensitivity experiment where the impact models were forced by the same climate change projections from HadGEM2-ES, RCP8.5 but coBut pCO$_2$ concentration was kept fixed at a "present day" reference level that differs from GGCM to GGCM (see Table 1). We will refer to this run as "fixed co2CO$_2$" run and indicate the associated crop yields by Y_{noCO2}. Y_{fixedCO2}. As a special case, the "default" simulations for pDSSAT do not use annual pCO$_2$ changes. Instead, pCO$_2$ was changed every 30 years using the average pCO$_2$ of the respective 30 year time slice.

For the analysis of the gridded data,

2.2 Effect of temperature change

We analyse the dependence of yield changes on ΔGMT separately for rain-fed and full-irrigation simulations, and for each cropare considered separately. Considering e. g., wheat yield changes under full irrigation. Since the timing of global warming differs between GCMs and scenarios, we group all available data into ΔGMT intervals (bins) separated by 0.5°C steps with 0.5°C width ($\pm$0.25°C around the central temperature), where ΔGMT is relative to the present day (1980–2010 average) reference level. For all annual data falling into a given interval and at one specific each grid point we apply a separate one-way analysis of variance (ANOVA fixed effects model) to individually calculate the variance explained by 1) different GGCMs, 2) the GCMs, and 3) the RCPs. The quantification of the RCP-dependence of the relationship between global warming and yield changes change is limited to a warming range up to 2 to 3°C above present depending on the GCM because only one RCP (RCP8.5) reaches temperatures above this threshold. However, we also provide the patterns of yield changes change for the higher concentration scenario. In the main text, all figures except Figure 1 9 & 10 refer to a ΔGMT level of 2.5°C(see Figure 1 for the associated years included) but the Supplement contains the figures for the other levels, and all figures except 3, 4, and 11 refer to crop model simulations driven by HadGEM2-ES climate. See Figure 1 for the years asso-

Table 1. Basic crop model characteristics with respect to 1) the implementation of CO2 CO_2 fertilization effect (as affecting radiation use efficiency (RUE), transpiration efficiency (TE), leaf level photosynthesis (LLP), or canopy conductance (CC)), 2) the accounting for nutrient constraints with respect to the CO2 fertilization effect and associated assumption with respect to fertilizer application (N = nitrogen, P = phosphorus, K = potassium), 3) implemented adaptation measures, and 4) starting conditions.

modelModel	CO_2 fertilization	Fertilizer useNutrient limitation	AdaptationStarting conditions
GEPIC (Liu et al., 2007; Liu, 2009)	RUE, TE pCO_2 of the fixed CO_2 run: 364 ppm	Limitation of potential biomass increase due to N stress (flexible N application based on N stress >10% up to an upper national application limit according to FertiStat (FAO, 2007)).Fixed present day FAO FertiStat database (FAO, 2007), fixed present-day P application rates following FAO FertiStatdatabase (FAO, 2007) FertiStat.	decadal adjustment of planting dates (incl. switch between winter and spring wheat); total heat units to reach maturity remain constantdecadal adjustment of winter and spring wheat sowing areas based on temperature present day
LPJ-GUESS (Lindeskog et al., 2013)	LLP, CC pCO_2 of the fixed CO_2 run: 379 ppm	no consideration of spatial and temporal changes in soil nutrient limitation	cultivar adjustments are represented by variable adjustment of total heat units to reach maturity (?), adjustments are based on the average climate over the preceeding during the preceding 10 years uncalibratedto keep growing season length constant
LPJmL (Bondeau et al., 2007)	LLP, CC pCO_2 of the fixed CO_2 run: 370 ppm	soil nutrient limiting factors are not accounted for no consideration of soil nutrient limitation	fixed sowing dates (Waha et al., 2012), ; total heat units to reach maturity remain constantpresent day (Leaf Area Index (LAI), the Harvest Index (HI), and a scaling factor that scales leaf-level photosynthesis to stand level are adjusted to reproduce observed yields on country levels.)
PEGASUS (Deryng et al., 2011)	RUE, TE pCO_2 of the fixed CO_2 run: 369 ppm	fixed N, P, K application rates (IFA, 2002)	adjustment of planting dates, ; variable heat units to reach maturity present day
pDSSAT pDSSAT (Jones et al., 2003; Elliott et al., 2014)	RUE, LLP, CC pCO_2 of the fixed CO_2 run: 330 ppm	fixed N present day present-day application rates	no adjustment of planting dates; total heat units to reach maturity remain constantpresent day

ciated with ΔGMT=2.5°C in HadGEM2-ES. The Supplement contains analogous figures for other GMT levels and GCMs.

We do not impose a specific functional relationship between global mean temperature change and changes GMT change and change in crop yields. Yield changes for any global mean temperature change for any GMT level between the central levels of the considered bins could be derived by a simple linear interpolation between the patterns of neighbouring bins but without assuming a linear relationship between global mean warming and yield changes change across the full range of warming.

2.3 Effect of pCO_2 change

The direct effect of CO_2 fertilization on crop yields is expected to introduce some scenario dependence in the relationship between GMT change and yield changeschange. We test to what degree the scenario dependence of the relationship can be explained by introducing atmospheric CO2 levels pCO_2 as an additional predictor for within-bin fluctuation of yields. To this end, we evaluate two different approaches to estimate the direct CO2 CO_2 effect on crop yields within the different GMT bins, described in detail in Section 3.2below. The two approaches differ in terms of the crop model simulations that they require: approach (a) only requires the default crop yield simulations with increasing pCO_2 whereas approach (b) requires a pair of simulations with increasing pCO_2 and with fixed pCO_2 at present-day reference level.

To evaluate and compare the performance of the two approaches we consider large scale regional average yields based on fixed present day (1998-2002)land use and irrigation patterns from MIRCA2000 (Portmann et al., 2010) and assess the reproducibility of the original RCP2.6, RCP4.5,

2.3.1 Approach (a)

For all years falling into a specific ΔGMT bin, approach (a) fits the following linear regression model to the response

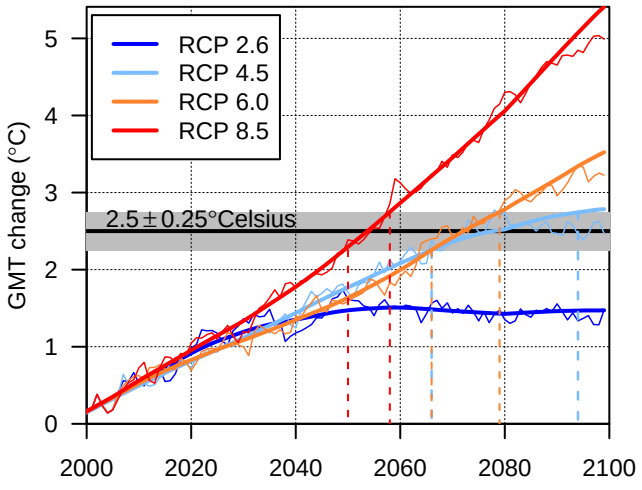

Figure 1. GMT projections from HadGEM2-ES for the four RCPs. The horizontal line and shading indicate the 2.5°C bin. The original annual GMT values (thin lines) are smoothed (thick lines) in order to obtain a contiguous time interval for each ΔGMT bin. The smoothing is based on a Singular Spectrum Analysis with a time window of 20 years (R-Package Rssa). E.g(R-Package Rssa, Korobeynikov, 2010; Golyandina and Korobeynikov, 2014; Golyandina et al., 2015). , years Years where the thick line falls within the shaded area are associated with ΔGMT = 2.5°C, and the corresponding time interval is delineated by the dashed vertical lines.

of yields in the default simulation to the increase in pCO_2:

$$\Delta Y_{\mathrm{varCO2}}(i,t) = \Delta Y_{\mathrm{clim}}(i) + a_1(i) \cdot (\mathrm{pCO2}(t) - 370\mathrm{ppm}) + \epsilon(i,t), \quad (1)$$

where $\Delta Y_{\mathrm{varCO2}}(i,t)$ is the absolute yield change in grid point i and year t with respect to the historical reference period (1980–2010) and $\mathrm{pCO2}(t)$ is the atmospheric CO_2 concentration of the corresponding year. In this statistical model, $\Delta Y_{\mathrm{clim}}(i)$ represents an estimate of the purely climate-induced yield change at the respective bin temperature, but assuming a fixed year-2000 pCO_2 of 370 ppm (i.e. without CO_2 fertilization), $a_1(i)$ represents the added effect of CO_2 fertilization, and $\epsilon(i,t) \backsim N(0,\sigma^2)$ represents the residual error.

2.3.2 Approach (b)

Approach (b) fits the following linear regression model to the yield difference between the default and fixed-CO_2 simulation for all years falling into a specific ΔGMT bin:

$$Y_{\mathrm{varCO2}}(i,t) - Y_{\mathrm{fixedCO2}}(i,t) = a_1(i) \cdot (\mathrm{pCO2}(t) - \mathrm{pCO2_{ref}}) + \epsilon(i,t), \quad (2)$$

where $Y_{\mathrm{varCO2}}(i,t)$ and RCP6.0 projections based on the emulated yield patterns (section 4) $Y_{\mathrm{fixedCO2}}(i,t)$ is the absolute yield in grid point i and year t of the default and fixed-CO_2 simulation, respectively, $\mathrm{pCO2}(t)$ is the atmospheric CO_2 concentration of the default simulation during the respective year and $\mathrm{pCO2_{ref}}$ is the crop-model specific pCO_2 value of the fixed-CO_2 simulation (see Table 1). In this statistical model, $a_1(i)$ represents the CO_2 fertilization effect and $\epsilon(i,t) \backsim N(0,\sigma^2)$ represents the residual error. No intercept is estimated in this model because yields from the default and fixed-CO_2 runs are expected to be identical if $\mathrm{pCO2}(t) = \mathrm{pCO2_{ref}}$. The purely climate-induced yield change at a fixed year-2000 pCO_2 of 370 ppm $\Delta Y_{\mathrm{clim}}(i)$ can then be derived as:

$$\Delta Y_{\mathrm{clim}}(i) = \Delta Y_{\mathrm{fixedCO2}}(i) + a_1(i) \cdot (\mathrm{pCO2_{ref}} - 370\mathrm{ppm}), \quad (3)$$

where $\Delta Y_{\mathrm{fixedCO2}}(i)$ is the average yield change in the respective warming bin of the fixed CO_2 simulation with respect to the historical reference period and $a_1(i) \cdot (\mathrm{pCO2_{ref}} - 370\mathrm{ppm})$ corrects for the different $\mathrm{pCO2_{ref}}$ used by each GGCM.

2.4 Emulator of temperature and CO_2 effects

Based on the spatial patterns of purely climate-induced yield change $\Delta Y_{\mathrm{clim}}(i)$ and added CO_2 fertilization effect $a_1(i)$, which are derived separately for each rain-fed and irrigated crop and specific to each crop model and GCM, we propose the following two-step interpolation method to compute crop yield changes for any given pair of ΔGMT and pCO_2, using either the coefficients from approach (a) or (b):

1. linear interpolation of $\Delta Y_{\mathrm{clim}}(i)$ between the two neighbouring warming bins to the desired ΔGMT value,

2. addition of the CO_2 pattern described by $a_1(i) \cdot (\mathrm{pCO2} - 370\mathrm{ppm})$, where $a_1(i)$ is also interpolated linearly between the respective coefficients from the neighbouring warming bins.

The application of these two steps using coefficients from method (a) above will be called emulator approach (a); their application using coefficients from regression method (b) will be called emulator approach (b). In addition, we propose a third, very basic emulator approach (c) where the yield change for any given ΔGMT is derived from a simple linear interpolation of the average yield change in the neighbouring warming bins of the default simulations $\Delta Y_{\mathrm{varCO2}}(i)$ with respect to the historical reference period, without using the associated pCO_2 as additional predictor.

The linear interpolation of any of the previous coefficients between two neighbouring warming bins is illus-

trated for a ΔGMT of 2.3°C as follows:

$$\mathrm{coef}(i, 2.3°\mathrm{C}) = (1-\delta)\cdot \mathrm{coef}(i, 2°\mathrm{C}) + \delta \cdot \mathrm{coef}(i, 2.5°\mathrm{C}),$$
$$\delta = (2.3°\mathrm{C} - 2°\mathrm{C})/(2.5°\mathrm{C} - 2°\mathrm{C}), \quad (4)$$

where coef can be $\Delta Y_{\mathrm{clim}}(i)$, $a_1(i)$, or $\Delta Y_{\mathrm{varCO2}}(i)$.

Using GGCM projections for the HadGEM2-ES climate input to train the emulators, we test which of the emulator approaches, (a), (b) or (c), provides the best reproducibility for yield changes simulated under the four RCPs (Section 4). While approach (b) requires a pair of crop model simulations – one with time-varying pCO_2 and one with fixed present-day pCO_2 – approach (a) and (c) only require the default simulations with time-varying pCO_2. Thus, a comparison of the three approaches could provide some important guidance regarding future crop model experiments required to allow for the proposed highly efficient emulation of crop model simulations. Since simulated crop yields are subject to considerable inter-annual variability, we also test what effect the amount of available training data has on the reliability of the derived regression coefficients. For that purpose, we train the emulators using either all available simulation data from the four RCPs or only simulation data from RCP8.5 and compare the fraction of the land surface for which derived fits are statistically significant as well as the difference between simulated and emulated yield changes. Due to the 30-year time slices of constant pCO_2 used by pDSSAT in the default run, approach (a) cannot be applied to this model using only RCP8.5 data. Since only RCP8.5 reaches ΔGMT$>$ 3.5°C this limits the temperature range of emulator approach (a) for pDSSAT even when using all available training data.

We evaluate and compare the performance of the three emulator approaches at the grid scale as well as the scale of large regions. Grid point yields (in t/ha) are multiplied by the fixed year-2000 crop-specific growing area from the MIRCA2000 dataset (Portmann et al., 2010) to derive regional total crop production (in t). MIRCA2000 provides gridded growing areas for a total of 26 rain-fed and irrigated crops based on a combination of census, remote sensing and other geographic data sources.

3 Mean Yield Change with Global Mean Temperature Change

3.1 Patterns of relative changes at different levels of global warming and main sources of variance

In general, increasing global mean temperatures correspond to an expansion of arable land to higher latitudes with concurrent yield reductions in equatorial regions. The highest positive changes in projected yields under rain-fed conditions at 2.5°C ΔGMT are typically in the northern high latitudes and mountainous regions for all crops (Figure 2Figure 2 for wheat, figures for other crops in the Supplement). These locations were previously inhibited by a short growing season, which extends with increasing air temperature (Ramankutty et al., 2002). Yield gains also occur over previously moisture limited regions, such as the northwestern U.S. and north-eastern China, in agreement with the findings of Ramankutty et al. (2002). In contrast, near the equator most crop yields decrease, especially maize and wheat. Since most cultivated land currently lies in low and middle latitudes, potential yield changes in those regions contribute a higher relative importance for today's food production system than changes in high latitudes.

While variations exist in the magnitude of projected yield changes, there is a high degree of consistency in the direction of yield change across ensemble members, especially over the high latitudes, where most of the largest projected yield changes occur, but where yields are in general smaller (Figure 3Figure 3). Utilizing output from all available combinations of one GCM, GGCM, and RCP scenario, more than three-quarters of the ensemble members indicate increasing crop yields over the upper mid latitudes in the northern hemisphere for all crops at 2.5°C.

The simulated yield values at each grid point and within each GMT bin are subject to variation due to the selection of impact model, GCM forcing, and emissions scenario. When considering all of these factors, the variance attributable to the impact model selection is much greater than that associated with the GCM or scenario choice in most regions (Figure 4Figure 4). This holds for rainfed rain-fed as well as irrigated simulationsand at all global mean warming bins above 1°C. The predominance of the impact model component in total variance is particularly evident in the middle to high latitudes for all four cereal considered crops, where impact model variance accounts for up to 90% of the grid point variance at 2.5°C.

3.2 Direct impacts of increasing pCO2pCO_2

In addition to air temperature warming, pCO2 pCO_2 has a direct influence on crop yields. As it varies within the different ΔGMT bins, it is expected to induce part of the fluctuations of the yield changes at given GMT levels. We find that this CO2 effect is not scenario dependent (see Figure 5 CO_2 effect shows little scenario dependence (see Figure 5 for the global average effect within the LPJmL simulations at ΔGMT=2.5°C), consistent with a short response time of plants to pCO2 changes.

pCO_2 changes. As expected, the CO_2-induced yield differences increase with heightened atmospheric CO2 CO_2 level under all emissions scenarios, implying a stronger CO2 CO_2 fertilization impact with increased pCO2. A least squares fit to the yield differences versus greenhouse gas level within each ΔGMT bin allows for a quantification of the direct CO2 effect at each level of warming based on global pCO2, rather than the emissions pathway. The underlying assumption is that the effect of the temperature variation within the 0.5°C range of each ΔGMT bin will be minimal compared to the effect of the CO2 variation across all RCPspCO_2.

To quantify the extent of the CO2 induced scenario dependence and its potential reduction at each grid point , we use two methods to determine the CO2 effect on crop

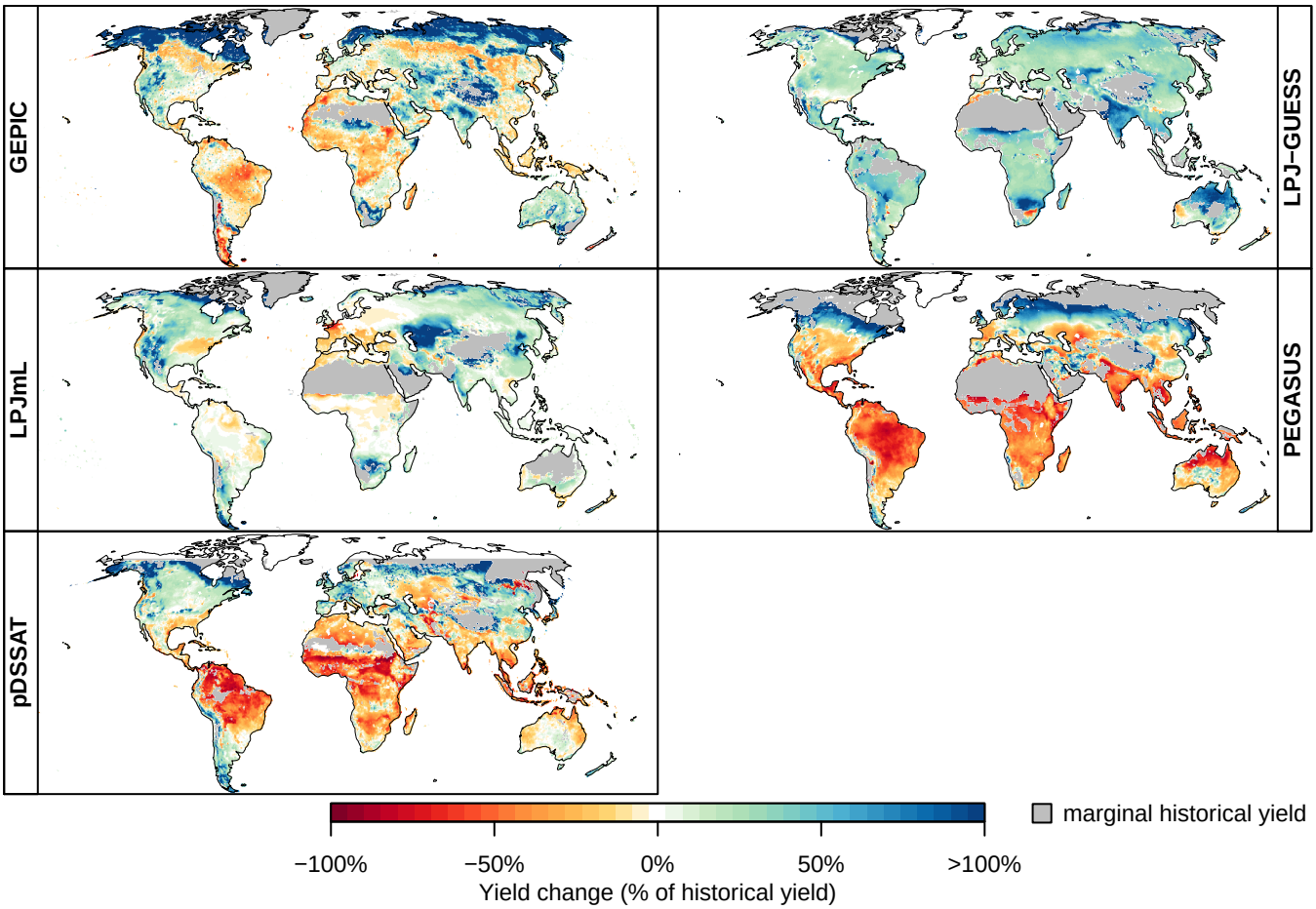

Figure 2. Average potential wheat yield change at ΔGMT=2.5°C as a percentage of the mean historical yield (1980–2010 average) under rain-fed conditions for each crop model forced by HadGEM2-ES. The average is calculated across all RCPs which reach the global mean warming interval from 2.25 to 2.75°C, namely RCP4.5, RCP6.0, and RCP8.5. Note that pDSSAT is run over a limited domain excluding areas north of 60°N. Regions with marginal historical yields (defined as lying below the 2.5% quantile of historical yields on year-2000 cropland) are masked to avoid exaggerated relative yield increases. Analogous figures for different crops, for irrigated conditions, as well as for absolute yield change (in t/ha) are available as supplementary online materialin the Supplement.

yields within each global mean temperature bin: By linear regression of absolute yield changes with respect to the historical reference period (ΔY_{CO2}) on

At the grid point level, two approaches have been used to separate purely climate-change-induced from CO_2concentration within the individual global mean warming bins, i.e. by fitting the following model where i indicates the individual year within the relevant ΔGMT bin, and $\epsilon_i \backsim N(0, \sigma^2)$ represents the residual error. The statistical model allows for the estimation of the purely climate-induced yield change ΔY_{CLIM} at a fixed year-2000 concentration of CO2 of 370 ppm. By linear regression of the within-bin differences between the default crop simulations (Y_{CO2}) and the fixed CO2 run (Y_{noCO2}) on the underlying CO2 concentration in the default simulation: where i indicates the individual year and $\epsilon_i \backsim N(0, \sigma^2)$represents the residual error. In this case the purely climate-induced yield change $\Delta Y_{CLIM}(\Delta GMT)$ is given by the yield change in the fixed CO2 run, ΔY_{noCO2}-induced yield change (following Equation 1 to Equation 3). Figure 6 shows the climate-change-induced yield change at ΔGMT), and an additive correction a_0. This correction accounts for the different levels of pCO2 in the fixed-CO2 run across different models; it is zero if the pCO2 in the fixed-CO2 run is 370 ppm.

=2.5°C for LPJmL under rain-fed conditions, using all available runs that fall into the warming bin to estimate $\Delta Y_{clim}(i)$. Figures for irrigated conditions and the other GGCMs are available in the Supplement. The two methods result in broadly similar patternsfor the climate change-induced relative yield changes (i.e., excluding direct CO2 fertilization effects), with yield increases in the high latitudes and upper mid- and high latitudes, mixed regions with decreases and increases in the lower mid-latitudes and mostly decreases in the tropicsand subtropics, broadly speaking (Fig. 6). However, the magnitudes of the changes are much larger with method magnitude of change differs between the two approaches: approach (a) (Fig. 6, lower panel). Some regional differences also occur between the two methodsgenerally estimates larger changes outside the tropics while yield decreases in the tropics are larger in approach (b). There are also some

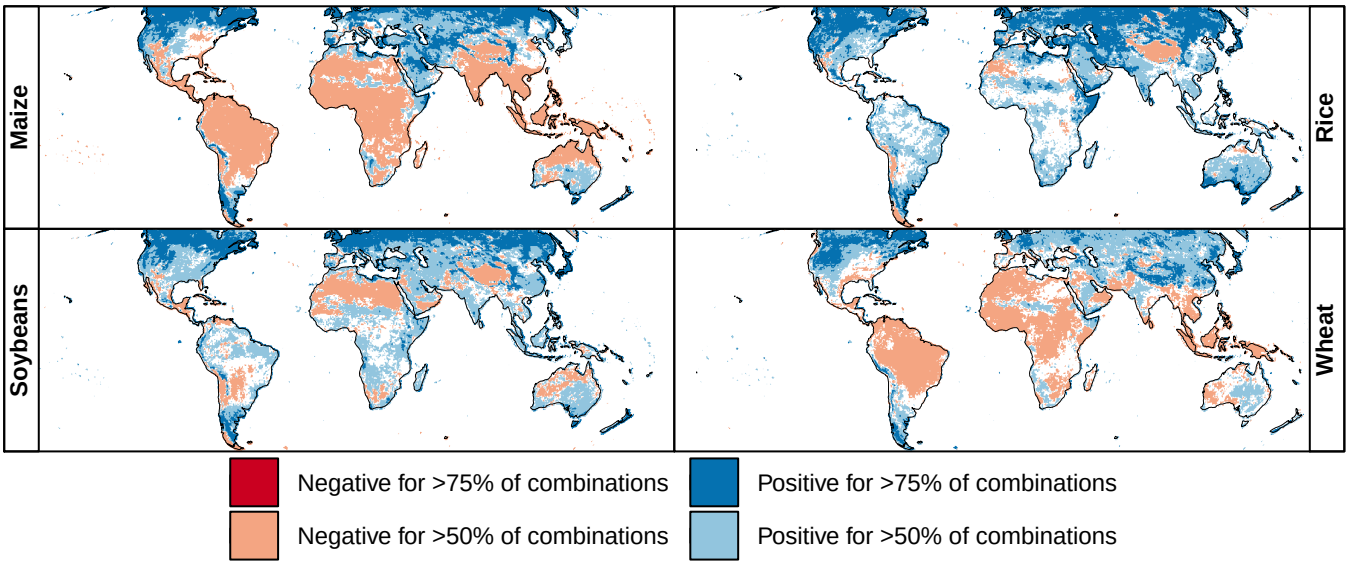

Figure 3. Percentage of crop model simulations (combination of a single GCM, GGCM, and RCP scenario) indicating an increase (blue) or decrease (red) in yield of greater than 5% at each grid point at 2.5°C warming scenario 2.5 ± 0.25°C ΔGMT as compared to the historichistoricalperiod for a) maize, b) rice, c) soybeans, and d) wheat under rain-fed conditions. White indicates either a less than 5% change or disagreement between the models in the direction of yield change. Note that only four out of five GGCMs provided results for rice. An analogous figure for irrigated conditions is available as supplementary online materialin the Supplement.

regions where both approaches disagree regarding the direction of change, such as for rice where there is disagreement on the direction of yield changes in southeast Asia .

In relative terms (estimated climate change-induced yield change divided by simulated present-day yield), both methods show very large values of frequently alternating sign in areas such as the Arabian peninsula or the northern Sahel (Fig. 6, upper panel). This is likely due to the very low present-day yield potential in these regions, leading to division by values close to zero. In the regional evaluation of the different emulator methods below, we will account for these regional differences in baseline yields by weighting potential yield changes by present-day growing areashigh latitudes of both Western North America and Eastern Russia for wheat and parts of Southeast and South Asia for all crops. Patterns of climate-induced yield change match better between both approaches under irrigated conditions.

In GEPIC, both approaches disagree on the direction of change for maize yields over large parts of Europe. In LPJ-GUESS, both approaches disagree on the direction of change in most of the tropics for all crops. While tropical yield change is predominantly negative in approach (b) mirroring results of the other crop models, approach (a) estimates mostly positive climate effects on tropical crops. In pDSSAT, approach (a) generally produces larger areas with negative yield change than approach (b). At the same time, positive yield effects in approach (a) have a larger magnitude than those in approach (b) in many regions. In PEGASUS, both approaches disagree on the direction of change over large parts of the U.S. for maize and soybeans, and large parts of China for wheat.

The estimates of CO2-induced yield changes CO_2-induced yield change also differ between the two methods (Figure 7). Method (b) results in a positive CO2 effect in most regions, except for some low-yielding areas and the potentially important cases of soybean in southern and eastern South America, and rice in north-west India and Pakistan, where it results in a negative effect of rising pCO2 on yield. With method approaches (Figure 7 for LPJmL results under rain-fed conditions). We expect CO_2 fertilization to have a positive or at least neutral effect on yields, and this is confirmed by approach (b) for all GGCMs and crops. Only GEPIC simulations show negative CO_2 effects on soybean and wheat yields in a few regions for approach (b). This can be explained by nutrient interactions in the model: CO_2 fertilization leads to yield increases first but also increases nutrient depletion in the soil compared to the fixed-CO_2 run. If fertilizer application is insufficient to replenish nutrient stocks this can lead to lower yields despite the beneficial effect of higher pCO_2. With approach (a), on the other hand, areas of negative estimated CO2 effect are much more widespread , and generally CO_2 effects are widespread in all GGCMs and all crops. Generally, the magnitudes of the estimated CO2 effect are again much largerthan with method CO_2 effect are also much larger, often surpassing those of approach (b) . As apreliminary conclusion, the results obtained with method (b) for the separate even in regions where the direction of change matches. Given that approach (a) contradicts our expectation of how CO_2 fertilization should affect yields in many regions we conclude that approach (a) is not reliable in separating the effects of climate change and pCO2 change on potential yields appear more realistic than those obtained with method (a).

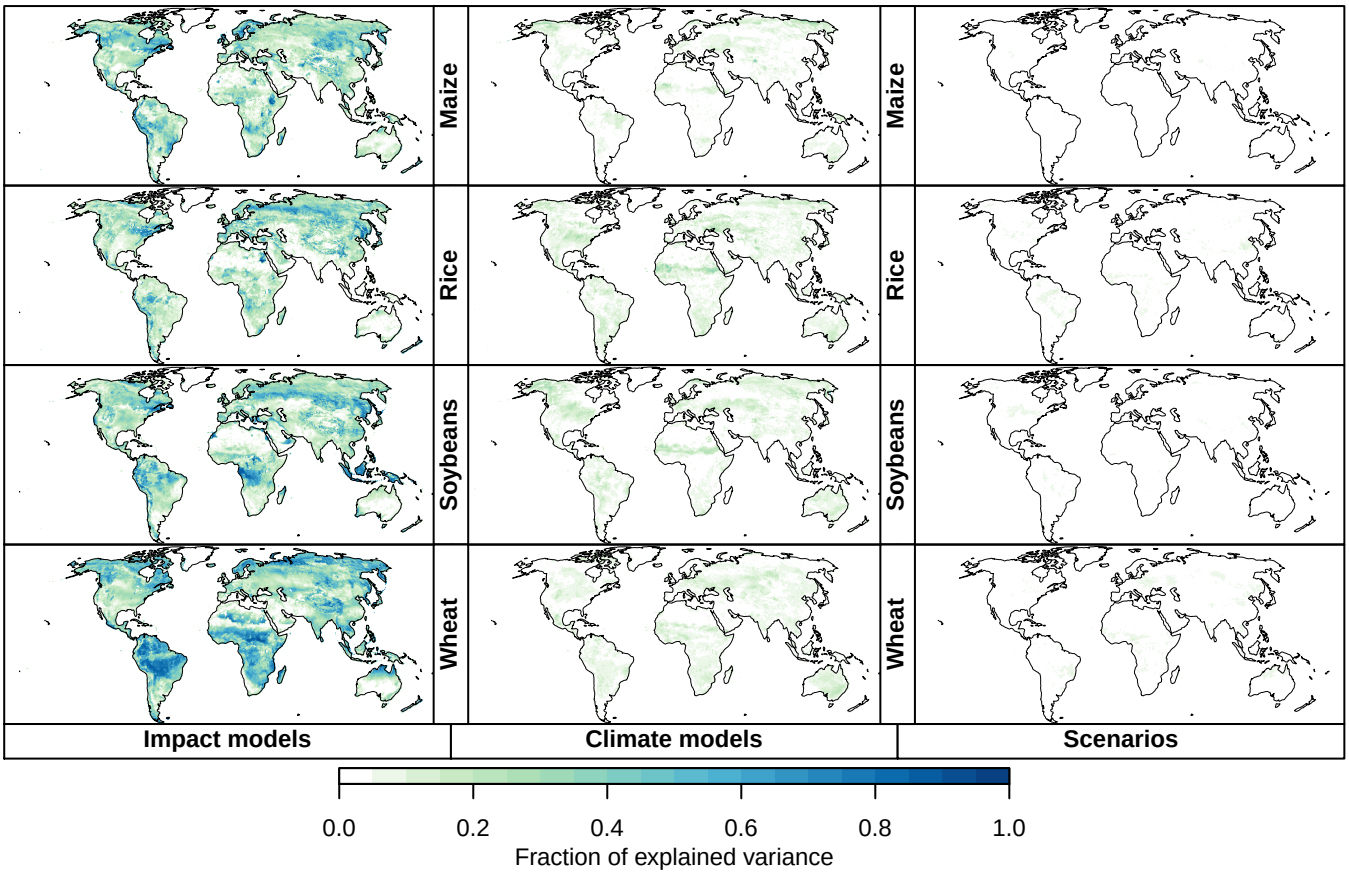

Figure 4. Fraction of total variance attributable to the impact models (GGCMs, left), climate models (GCMs, middle), and scenarios (RCPs, right) for each crop. Figure shown for rain-fed runs at ΔGMT=2.5°C $\Delta GMT = 2.5 \pm 0.25°C$ warming; an analogous figure for irrigated runs is provided as supplementary online materialin the Supplement.

4 Validation of three emulator approaches

Based on the on yield from those of pCO_2 change. By design, climate-induced patterns (assuming fixed year 2000 levels of CO2) of relative yield changes and the associated within-bin relationship between CO2 and crop yields identified in section 3, we propose the following two-step interpolation method to compute crop yield changes for any given pair of ΔGMT and pCO2, using either of the above regression methods (a) or (b) : Linear interpolation between the temperature-specific, CO2-adjusted yield patterns of neighboring ΔGMT bins ($a_0(\Delta GMT)$ from method and CO_2-induced yield changes add up to the full yield change (see Equation 1) which is why the difference between the patterns of estimated CO_2 effect explains why climate-change patterns from Figure 6 also differ substantially between both approaches in some regions. Approach (a) or $Y_{noCO2}(\Delta GMT)$ + $a_0(\Delta GMT)$ from method (b))to the desired ΔGMT value Addition of the CO2 pattern described by a_1 * (has a structural disadvantage to approach (b) in that it estimates both the climate-induced and CO_2-induced effect on yields from the same linear regression model (Equation 1). Besides changes in pCO_2 annual yields in each warming bin are subject to substantial inter-annual climate variability which means that individual years with a higher pCO_2 do not necessarily have a higher yield. In contrast, approach (b) only estimates the CO_2– 370ppm) , where the pattern of scaling coefficients a_1 is also interpolated linearly between the scaling coefficients from neighboring temperature bins The application of these two steps using regression method (a)will be called emulator -induced yield change from the regression model (Equation 2) while both the default and the fixed-CO_2 run are subject to identical climate variability. There is inter-annual variability in the CO_2-induced yield change as well (see Figure 5 for the global average effect), however, it is much smaller than the total yield variability. While approach (a) ; their application using regression method (b) will be called emulator approach and (b) . In a third, very basic emulator approach (c), crop yield change patterns for a given should provide similar estimates of the CO_2-induced yield change given a large sample, our sample size is limited by the number of years falling into each ΔGMT level are derived from an interpolation between the two neighboring ΔGMT bins' average patterns; where these average patterns are derived from the bin (Table 2). This number varies between seven years in the 4.5 and 5.0°C bin and up to 66 years in the 1.0°C bin when yield data from all RCPs are used to train the emulator. The number of years varies between seven and 13 years if only data from RCP8.5 projections of the individual climate and

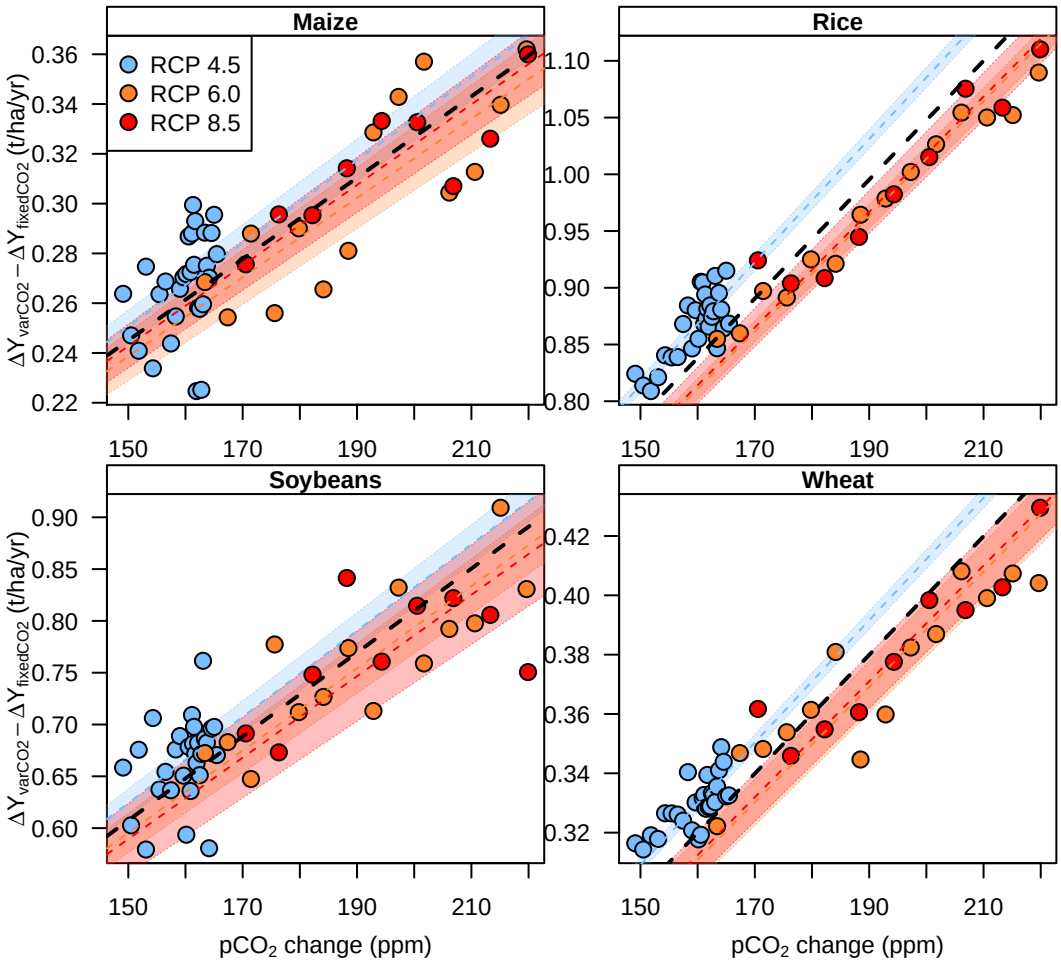

Figure 5. Difference in global mean yield change (sum of rainfed rain-fed and irrigated, and weigthed weighted by present-day year-2000 growing areas) between the default ($Y_{CO2varCO2}$) and fixed CO2 CO_2 simulations ($Y_{noCO2fixedCO2}$), for each crop over the range of pCO2 pCO_2 associated with the ΔGMT=2.5°C bin. Results are as simulated by LPJmL forced with output from HadGEM2-ES. Each color represents an emission scenarioand black . Points mark individual years while dotted lines and shaded areas indicate the linear best fit and its 95% confidence interval for each cropscenario. The black dotted line indicates the linear best fit through all available scenarios. Analogous figures for other GGCMs and warming bins are available in the Supplement.

crop model simulations accounting for the CO2 fertilization effect. E. g. to derive the crop yield change pattern for a global mean warming of 2.3are used. Given the limited sample size and possibly large variability, the derived fits are often not statistically significant. For approach (a) we found that derived fits were rarely significant on more than 25% of the crop-specific growing area (Portmann et al., 2010) using a p-value of 0.05 (figure available in the Supplement). Values were even lower if only RCP8.5 was used for the regression. In contrast, fits derived by approach (b) were mostly statistically significant ($p < 0.05$) on more than 70% of the growing area, often on more than 90% of the area. We also found only a small negative effect in terms of statistical significance if only RCP8.5 was used in approach (b).

4 Validation of three emulator approaches

Using GGCM projections for the HadGEM2-ES climate input, we test which of the approaches, (a), (b) or (c), provides the best reproducibility for RCP2.6, RCP4.5, and RCP6.0 when estimates of the climate-induced and CO2-induced effects are based on RCP8.5 projections. While approach (b) requires a pair of crop model simulations – one with time-varying pCO2 and one with fixed pCO2, approach (a) only requires the default simulations with time-varying pCO2. Approach (c) assumes that yield changes can be estimated using only all four RCPs. For that purpose, we apply each emulator with time series of ΔGMT as a predictor without consideration of the associated pCO2. Thus, a comparison of the three approaches could provide some important guidance regarding future crop modelexperiments required to allow for GMT and pCO_2 from the RCPs and compare emulated yield changes in each grid point and as well as total crop production for 10 large world regions to those simulated by

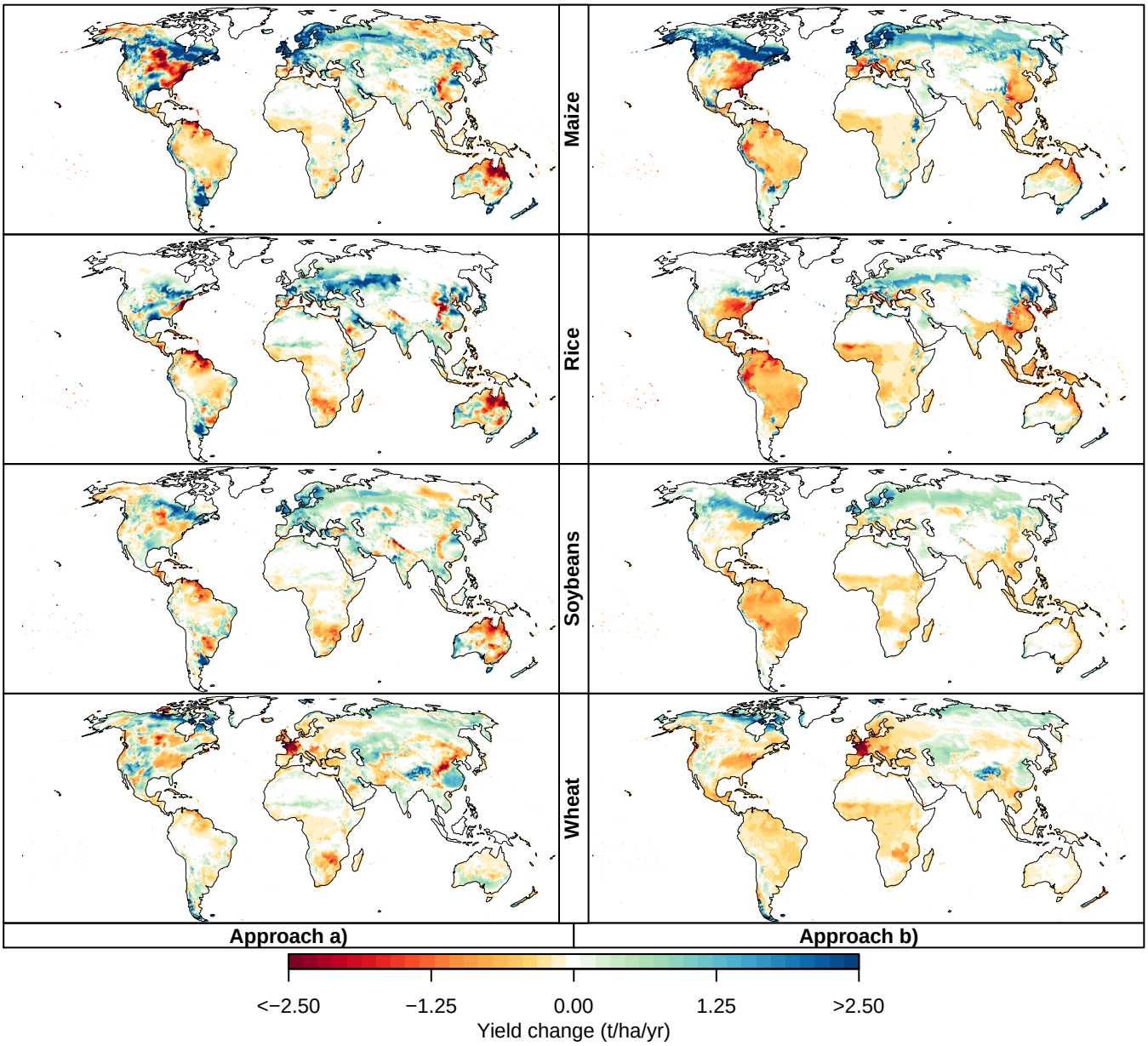

Figure 6. Climate change-induced yield changes at ΔGMT=2.5°C of global warming and year 2000 pCO_2 level (370 ppm). Left column: Patterns of $\Delta Y_{\mathrm{clim}}(i)$ derived at each grid point i by approach (a) (see Equation 1). Right column: Corresponding patterns of $\Delta Y_{\mathrm{clim}}(i)$, derived by approach (b) (see Equation 3). Both types of patterns are derived from LPJmL simulations forced by HadGEM2-ES assuming rain-fed conditions and expressed as absolute differences compared to the historical period (1980–2010). Rows: Different crop types. Analogous figures for irrigated conditions, for different GGCMs, and using relative instead of absolute yield changes are available in the Supplement.

Table 2. Number of years of yield data available in each ΔGMT bin for HadGEM2-ES. Only RCP8.5 reaches warming levels above 3°C.

Data used	**ΔGMT bin**									
	0.5°C	1.0°C	1.5°C	2.0°C	2.5°C	3.0°C	3.5°C	4.0°C	4.5°C	5.0°C
all available scenarios	47	66	44	38	52	20	8	8	7	7
RCP8.5 only	10	13	12	10	9	8	8	8	7	7

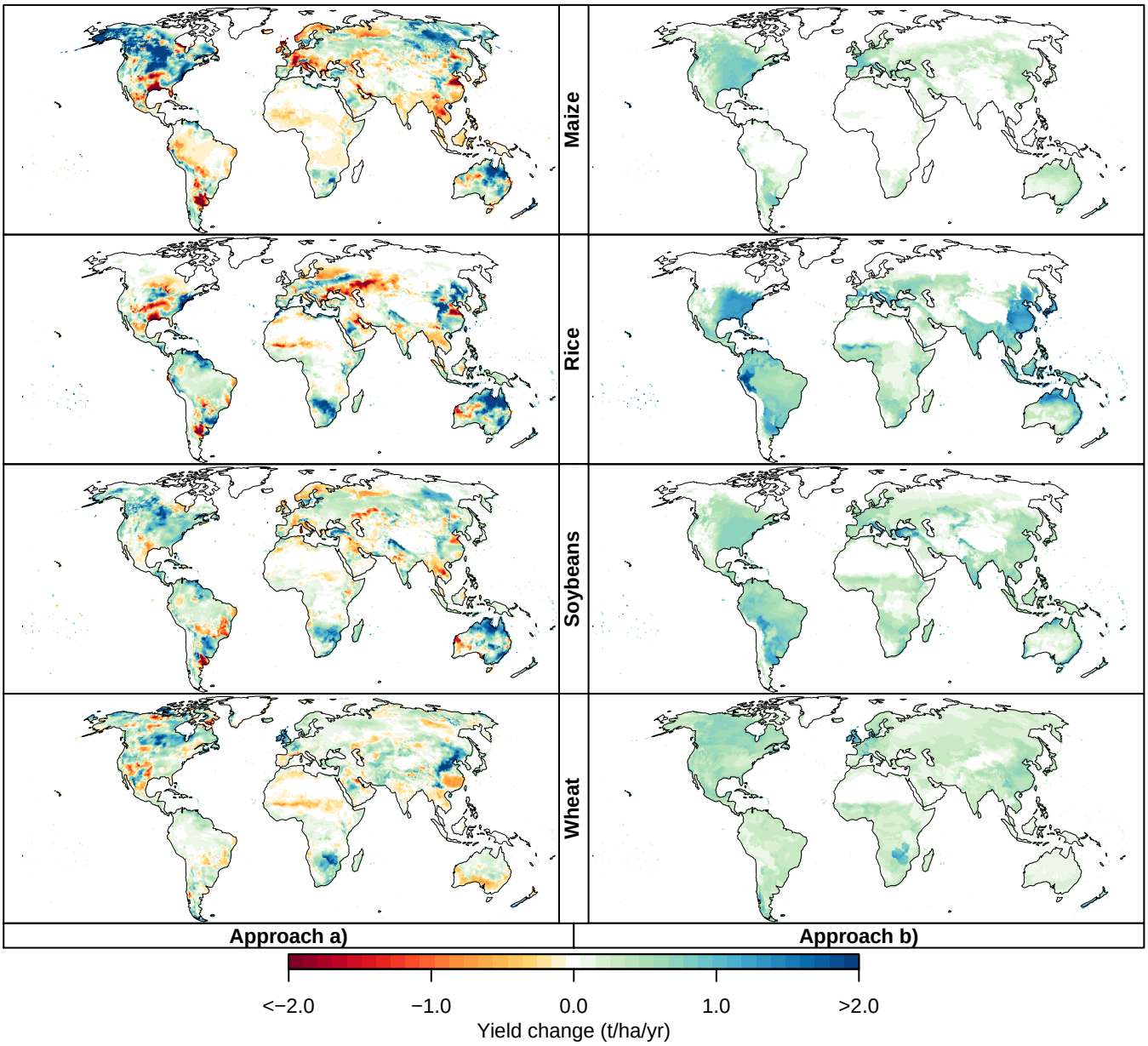

Figure 7. CO_2-induced yield changes at 2.5°C of global warming for LPJmL forced by HadGEM2-ES assuming rain-fed conditions. Analogous to Figure 6, but showing the scaling coefficients $a_1(i)$ from approach (a) (left column) and approach (b) (right column), multiplied by the average pCO_2 change compared to year 2000 (370 ppm) across all years falling into the GMT bin. Rows: Different crop types. Analogous figures for irrigated conditions, for different GGCMs, and using relative instead of absolute yield changes are available in the Supplement.

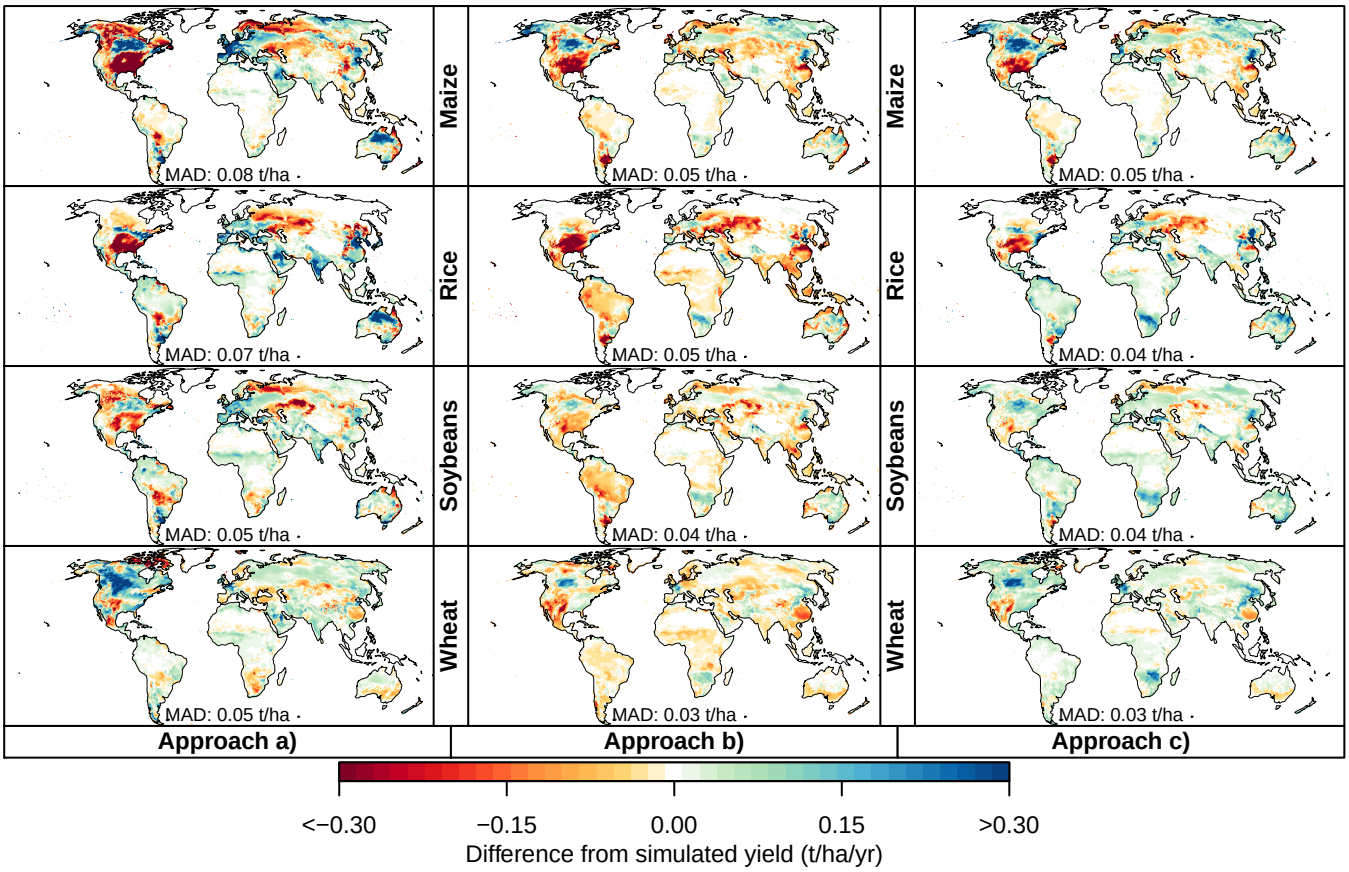

Figure 8. Validation of the three emulator approaches. Maps show the difference (emulated minus simulated) between the simulated LPJmL yields forced by HadGEM2-ES climate for RCP4.5 under rain-fed conditions for all years falling into the ΔGMT bin of 2.5°C (2066–2094) and the emulated yields for the same years based on approach (a) (left column), approach (b) (middle column), and approach (c) (right column). Rows: Different crops. MAD: mean absolute difference, regardless of sign, averaged across all grid points. Analogous figures for irrigated conditions and for different GGCMs are available in the Supplement.

the GGCM. For pDSSAT, the proposed highly efficient emulation of crop model simulations. pCO_2 time series used in that model's default run is also used with the emulator.

Figure 8 shows results for the LPJmL model, when applying the emulators trained on all available data to reproduce rain-fed yields under RCP4.5. Figures for other RCPs, irrigated yields and other GGCMs are available in the Supplement.

Approach (a) generally leads to the largest differences relative to the simulated yield change (Fig. 8Figure 8, left column). In particular Maize, rice, and soybean yields are underestimated for much of North America, and overestimated in Europeand South America, temperate South America, and Australia. Wheat yields are overestimated, e.g.in Canada. These discrepancies are mainly due to the climate-change effect estimated by approach (a) (cf. Figure 6), whereas the CO2 fertilization effect even points in the opposite direction in many of these regions (cf. Figure 7). In fact, we note again that approach (a) estimates the CO2 fertilization effect to be negative in some regions (Figure 7), which is not consistent with theory and empirical evidence, in Canada.

Approach (b) also leads to some substantial deviations from the potential yields simulated by LPJmL, in percentage terms, mainly in the northern hemisphere and in Australia (Figure 8, top panel(Figure 8, middle column). But large relative differences are mainly found outside the major growing regions of the respective crop, in areas where absolute potential yields are low today. Correspondingly, absolute differences between the LPJmL simulations and the emulator Spatial patterns of over and underestimation are broadly similar to approach (a), but the magnitude of the difference is generally slightly lower. In the tropics, approach (b) are modest (Figure 8, bottom panel, middle column). An important exception is the underestimation of simulated maize and rice yields in southern North America. We note that LPJmL itself has limitations in simulating yield variability in this region (Frieler et al., 2017). often leads to a higher deviation from the simulated yields than approach (a), particularly for rice and soybeans in South America.

Finally, approach (c) leads to a similar pattern of deviations from the simulated yield potential yields as approach (b) , but with a slightly smaller magnitude (Figure 8for maize (Figure 8, right column). Thus, considering overall performance at the grid point level for this particular case (2.5°C warming under RCP4.5) , the simple For the other crops,

approach (c) often leads to an overestimation of yields whereas approach (b) tends to underestimate simulated yields. The average deviation between emulated and simulated yields (designated as MAD in Figure 8) is similar for approach (b) and (c). Approach (c) performs slightly better than approach (b) for rice, and both approach (b) and (c) perform better than approach (a) for all four crops. Differences between the three emulators are smaller when reproducing RCP6.0 and RCP8.5 (figures available in the Supplement).

The difference between emulator approach (c) produces results which are closest to the LPJmL simulation. b) and (c) is even smaller in the other crop models than in LPJmL (figures available in the Supplement). Overall, MAD between emulated and simulated yields is up to 50% higher than LPJmL in PEGASUS, roughly twice as high in GEPIC and up to three times as high in pDSSAT. In LPJ-GUESS, MAD between emulated and simulated yields is similar for all three emulator approaches, even though the spatial patterns of over and underestimation differ.

Using only RCP8.5 instead of all available data to train the emulators has a detrimental effect on the performance, especially for approach (a). MAD between emulated and simulated yields increases by a factor of more than three, even close to four for some GGCMs and crops, under RCP4.5. MAD for approach (b) and (c) also increases by a factor of more than two, although not as sharply as for approach (a) (figures available in the Supplement). Performance loss is lower for RCP6.0, with MAD generally less than twice as high. The emulator trained on RCP8.5 alone shows better performance in emulating RCP8.5 simulated yields than the emulator trained on all available data.

To get a more comprehensive indicator indication of the performance of the emulator for the whole 95-year time series (instead of just the 2.5°C bin) we use all three approaches to reproduce the simulated changes in crop production under RCP2.6, RCP4.5, and RCP6.0, and RCP8.5, as derived for 10 large scale world regions (cf. Figure 2 in Lotze-Campen et al. (2008) see Figure 10 for a map of the regions). . Grid-point yields are aggregated to the regions assuming fixed year-2000 land use and irrigation patterns. Compared to potential gridded yields, using production gives less weight to areas where a crop is not currently grown. The climate-induced and CO2-induced patterns of change were derived from RCP8.5; and we used the RMSE between the relative changes in crop production derived from the original simulations and their emulated counterparts across the other three scenarios Since none of the emulators is expected to capture the relatively large inter-annual variability of simulated yields we compare simulated and emulated decadal production and calculate the RMSE over all decades of the relative difference between emulated and simulated decadal production (in %) as a measure of the performance of the emulator.

Of the two approaches that estimate warming and CO_2-induced effects separately, approach (b) generally provides a better performance than approach (a) (see Figure 9 Figure 9 for LPJmL; Table 1 and supplementary online information Table 3 and the Supplement for all crop models). Performance of all emulator approaches varies substantially between regions. There are also considerable differences between crop models. For LPJmL, emulator approach (b) generally provides marginally better performance for many regions than approach (c)when emulating RCP2.6 and RCP4.5. This advantage of approach (b) is not found in . However, this is not consistent across the emulators for the other crop models. Taking into account that approach (b) requires additional crop model simulations with fixed CO_2 and that performance is mostly very similar for approach (b) and (c), the very basic interpolation approach (c) may appears toprovide the best compromise between emulator performance and complexity.

While none of the emulators is expected to capture the relatively large inter-annual variability of simulated yield changes, approach (c) allows to emulate the regionally averaged response of the process-based crop models to climate forcing estimated for RCP2.6, RCP4.5, and RCP6.0 (Fig. 10 for maize yields from LPJmL forced by HadGEM2-ES; analogous figures for other combinations are available as supplementary online material). Note though that the average deviation difference between emulated and simulated yields production over the full 95-year time series is sometimes larger than the simulated yield production change in 2091–2099, especially in the low warming scenarios (marked by red crosses in Fig. 9) Figure 9). Table 3 compares the RMSE between emulated and simulated crop production in the largest producing region of each crop for all five crop models.

Figure 10 illustrates the performance of emulator approach (c) in reproducing decadal maize production as simulated by LPJmL forced by HadGEM2-ES. Emulated yields generally follow the simulated trends, although large errors exist, e.g., in North America, which also stands out in Figure 9 and Figure 8. Analogous figures for all crops, emulator approaches and crop models are available in the Supplement.

Similar to the grid point results, using only RCP8.5 to train the emulators leads to a performance loss for all emulator methods and all RCPs except RCP8.5. This performance loss is larger for approach (a) than approach (b) and (c), and is generally highest for RCP4.5 (figures available in the Supplement).

5 Increases in Regional Crop Yield Variance

In addition to estimating the yield changes change associated with a rise in average temperature, it is important to consider the implications of rising variance. Climate change is expected to increase not only the average temperature, but to impact the variance of temperature and precipitation, including an increase in the frequency and duration of extreme events. For this reason, when deriving simplified relationships between potential yields yield change and global climate change, it is crucial to account not only for the mean effects of rising temperature, but also their concurrent implications

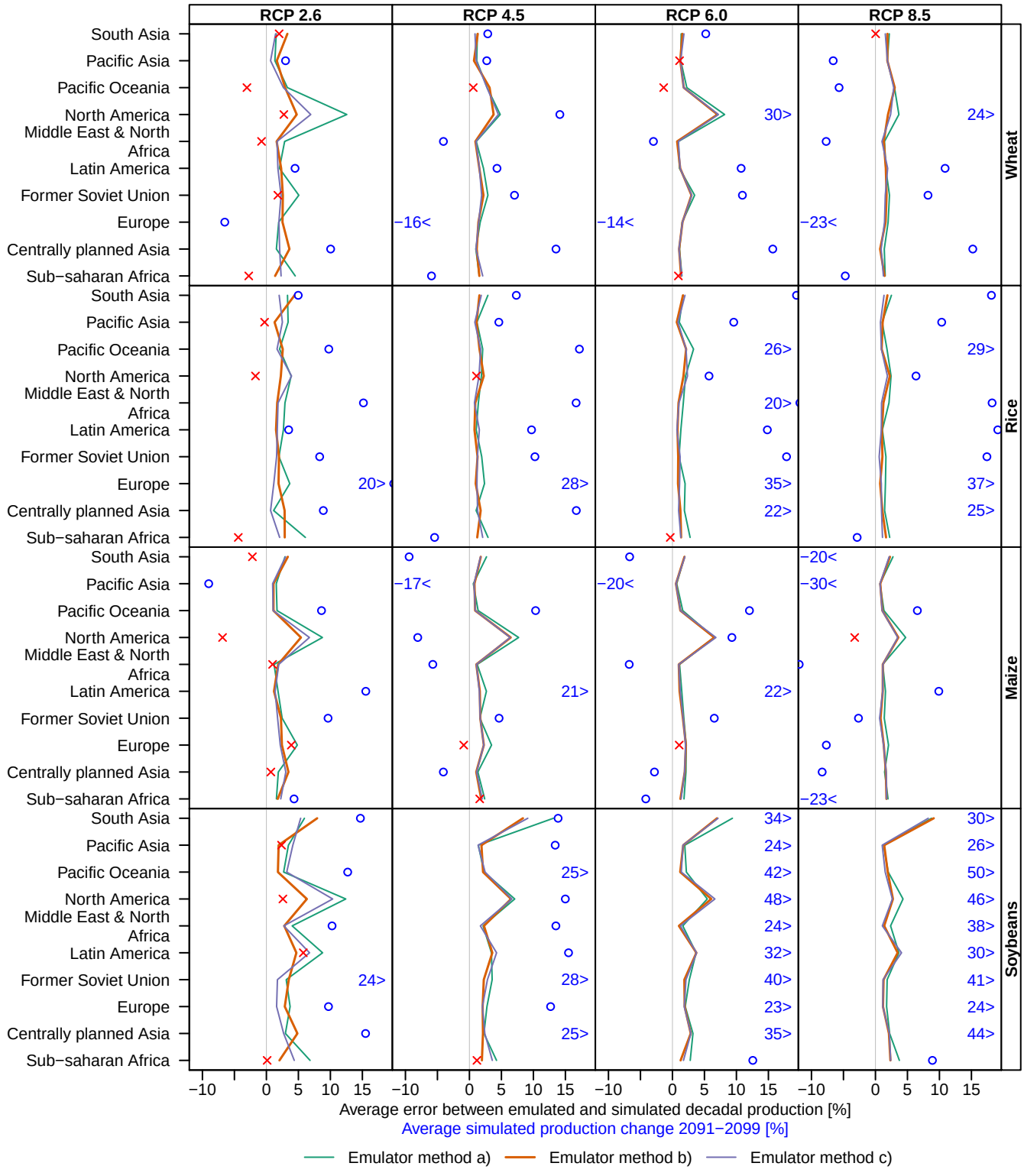

Figure 9. Root mean square difference (in %) between emulated and simulated regional decadal production (yields multiplied by year-2000 growing areas, combined for irrigated and rain-fed crops) for LPJmL forced by HadGEM2-ES climate projections. The emulator was built using all available data and used to reproduce yield changes in all four RCPs. For comparison, point symbols illustrate the average simulated yield change for 2091–2099 (same horizontal axis), using red crosses or blue circles depending on whether the error between emulated and simulated production is larger or smaller than the simulated change. Analogous figures for the other crop models are available in the Supplement.

Table 3. Average root Root mean square deviation difference between emulated and simulated decadal production (expressed in % of the simulated production as in Fig. 9Figure 9) in the largest producing region of each crop, for all five crop models forced by HadGEM2-ES climate projections. Average over across all four RCPs. The values for all combinations of models, crops, and regions, and separately for each RCP, can be found in the supplementary online materialSupplement. Top: emulators trained on all available data; bottom: emulators trained on RCP8.5 only.

(a) Emulators trained on all available data

Model	Wheat, Europe			Rice, South Asia			Maize, North America		
method heightApproach	a	b	c	a	b	c	a	b	c
GEPIC	1.334	1.267	1.215	3.982	3.037	2.790	10.099	9.058	9.360
LPJ-GUESS	2.242	2.254	2.213	4.033	2.163	3.729	5.870	5.466	5.359
LPJmL	1.777	1.768	1.596	2.582	2.371	1.786	6.923	5.494	5.846
pDSSAT[1]	5.363	3.196	3.550	7.758	3.606	4.190	12.218	6.129	6.149
PEGASUS	6.061	4.908	4.937	n.a.	n.a.	n.a.	8.762	8.533	8.496

(b) Emulators trained on RCP8.5 only

Model	Wheat, Europe				Rice, South Asia				Maize, North America			
Approach	a	b	c		a	b	c		a	b	c	
GEPIC	2.159	1.250 1.309	1.396		6.941	3.321 3.541	3.266		19.091	10.310 9.779	9.664	
LPJ-GUESS	2.579	2.348 2.449	2.486		5.026	2.614 2.656	4.517		10.034	7.029 7.083	6.866	
LPJmL	3.814	2.272 2.293	2.415		4.247	2.954 3.040	2.409		11.954	5.783 5.838	5.950	
pDSSAT	4.863 n.a.	4.495 4.053	4.392	6.483	5.232 n.a.	4.230	4.971	12.752	8.065 n.a.	8.290	7.984	
PEGASUS	8.125	4.923 5.167	5.324		n.a.	n.a.	n.a.		14.097	11.829 11.801	11.825	

[1] Emulator approach (a) for pDSSAT only covers warming up to 3.5°C, i.e. up to 2070 under RCP8.5.

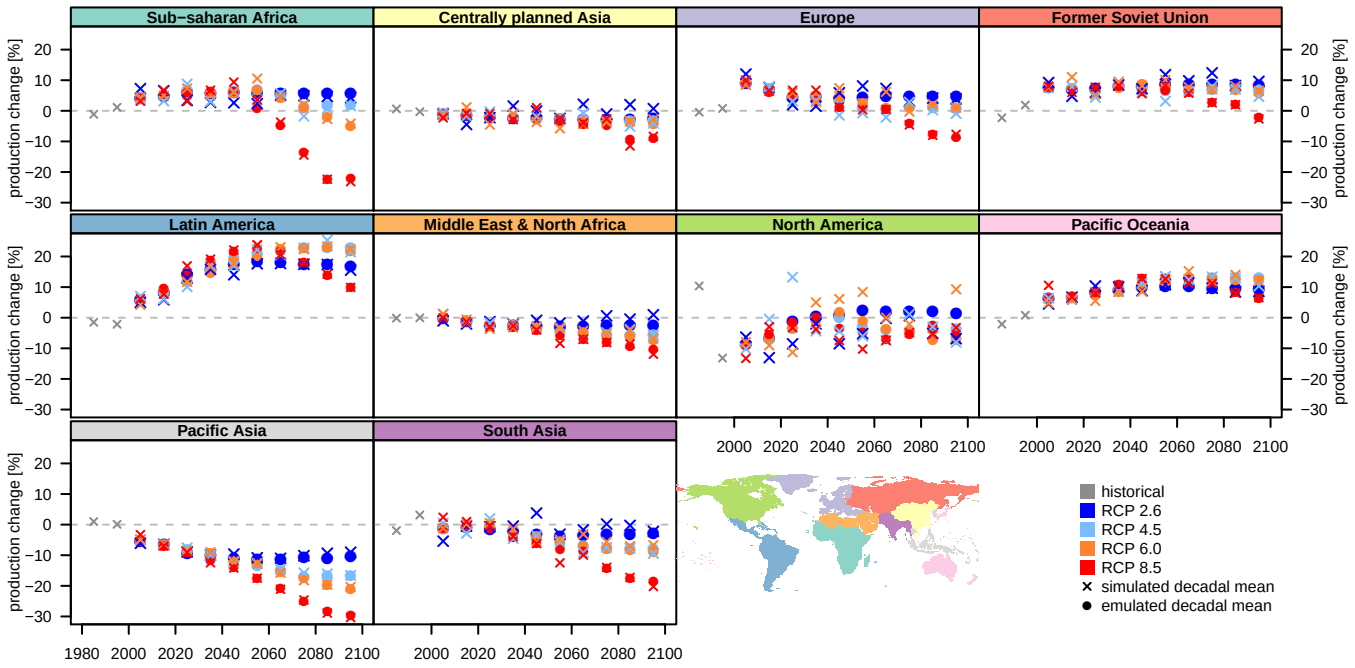

Figure 10. Comparison of simulated and emulated time series of regionally averaged aggregated crop production changes for LPJmL forced by HadGEM2-ES climate projections. Regional averages are calculated based on fixed present day land use and irrigation patterns. Results are shown for Maize and emulator approach (c).

for crop yield variance. Interannual Inter-annual yield variance can be computed for the same 0.5° C warming bins as used above for the average yields, which we do here for all major four crops under the "no irrigation" scenario. To account for the variability across scenarios and models which is attributable to direct CO2 effects, the The variance is calculated separately for the years of each RCP-GCM-GGCM specific mean is subtracted at each 0.5combination falling into the 2.5°C ΔGMT step. The variance of the adjusted yields is then compared to the warming bin and compared to thevariance of the same matching GCM-GGCM combination over the historical period (1980–2010)period.

The global figures show broadly similar patterns across all four crops: Increases increases in yield variability in much of the northern hemisphere, particularly in North America, central Asia, and China; as well as in the southern mid-latitudes (Figure 11 for 2.5°CFigure 11). A majority of model combination projects decreasing variability in tropical regions (except for rice) as well as parts of Eastern Europe; but nowhere do more than 75% of the model combinations agree on a decrease in variability. In several instances increased variability occurs in highly productive regions such as in China for rice and the US, Brazil, and Argentina for soy. Wheat also has an increased variability in more than 7550% of the crop model simulations over the highly productive regions in China and the U.S. Such an increase in variability, if realized, could manifest as impacts on the price, whose volatility is tightly linked to rapid changes in supply (Gilbert and Morgan, 2010).

6 Summary

Evaluating the impacts of climate change at different levels of global warming, and thus evaluating mitigation targets, requires a functional link between ΔGMT and regional impacts. Here we have shown that changes in crop yields, as simulated by gridded global crop models, can be reconstructed based on ΔGMT, with some limitations. The small spread of simulated yield change across the RCP scenarios as compared to the GCMs and impact models implies that projected impacts at different ΔGMT levels are not substantially dependent on the choice of emissions pathway. In this context, it has to be noted that the scenario setup of the ISIMIP crop model simulations was chosen specifically to minimize scenario-dependency by asking modellers to keep crop management fixed at present-day level or adjust it only in response to climate without any regard to the time horizons associated with adaptation or economic processes. Four models are calibrated to match present-day yield levels while LPJ-GUESS simulates potential yields assuming optimal management. Only two of the crop models allow for an adjustment of planting dates in response to climate change (GEPIC and PEGASUS, see Table 1). Three of the models keep the total heat unit sum to reach maturity constant, assuming no change in crop cultivar which effectively leads to a shortening of the growing season. Representation of soil nutrient limitation varies substantially between models, with two models (LPJ-GUESS and LPJmL) considering no soil nutrient limitation at all, while the nutrients considered and the assumptions on fertilizer application differ between the other three models. The effects of these assumptions on yield changes simulated by the different crop models are not studied here since the focus of this study is on developing efficient emulators, but these assumptions inform both the simulated yield changes as well as the emulators which attempt to imitate the behaviour of the crop models. The results of the ISIMIP crop models have been studied in detail in Rosenzweig et al. (2014).

We have tested three different approaches for emulating crop yield changes simulated by GGCMs, two of which include pCO2 change simulated by five GGCMs driven by HadGEM2-ES climate projections for four RCPs. All approaches rely on ΔGMT as the main predictor of yield change at the grid scale. Two of the approaches include pCO_2 as an additional predictor. An approach (a) attributing the yield variation within an individual ΔGMT bin of a simulation with varying pCO2 pCO_2 solely to the change in pCO2 pCO_2 shows the poorest overall performance. An approach (b) based on the difference between runs with and without direct CO2 CO_2 fertilization effects performs similarly well as a simple approach (c) using only ΔGMT as a single predictor. For local (grid level)crop yields, Considering the added complexity in approach (b) compared to (c), the simple approach (c) performs slightly better than approach (b) for the LPJmL GGCM. On the other hand, appears in general preferable even though it may not provide the best result in all regions. While our tests indicate that the emulators perform better for some crop models than for yield changes weighted by actual growing areas and irrigation patterns and aggregated over large regions (i.e., regional production) , approach (b) slightly outperforms approach others we strongly advise against relying solely on results from any one particular model, but instead to always consider the full range of uncertainty spanned by the GGCMs. Similarly, different GCMs still account for more than 15% of the total variance of the ISIMIP ensemble at ΔGMT=2.5°C in a number regions (Figure 4) which is why emulators should be constructed for all GCMs.

Given the availability of crop model simulations in the ISIMIP archive, emulators based on approach (a) and (c) in reproducing changes under low-warming RCPs. Considering the added complexity in could be constructed for all five GGCMs for the remaining four GCMs (IPSL-CM5A-LR, MIROC-ESM-CHEM, GFDL-ESM2M, NorESM1-M). Emulators based on approach (b) compared to (c), the simple could only be constructed for LPJmL and pDSSAT (and PEGASUS if using only RCP8.5 for training). With its five GCMs, which were selected from the CMIP5 ensemble based primarily on data availability at the time, the ISIMIP subset likely underestimates the total uncertainty in future climate impacts attributable to GCMs for many regions, however, the ISIMIP subset es-

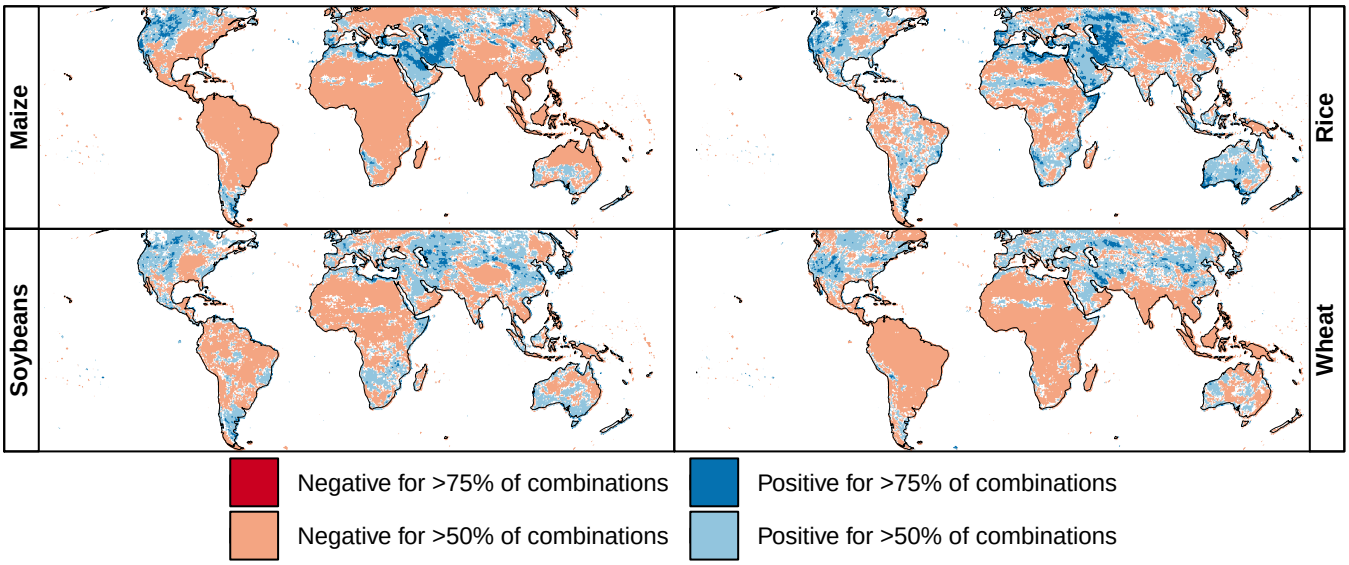

Figure 11. Percentage of crop model simulations (combination of a single GCM, GGCM, and RCP scenario) in the 2.5°C warming bin indicating an increase (blue) or decrease (red) in yield variance of greater than 5% at each grid point at 2.5°C warming scenario as compared to the historichistoricalperiod for a(1980–2010), for maize, b) rice, c) soy, and d) wheat under rain-fed conditions. White indicates either a less than 5% change or disagreement between the models in the direction of change. Note that only four out of five GGCMs provided results for rice. An analogous figure for irrigated conditions is available in the Supplement.

sentially samples as much uncertainty as is possible with only 5 GCMs (McSweeney and Jones, 2016). The generally good performance of approach (c) appears in general preferable. This suggests that simplified predictions of large-scale agriculture agricultural yields may not require additional crop model simulations with CO_2 levels held at a historical level if planning to extend the GCM coverage.

The impact model ensemble available with ISIMIP data assembled in this study also indicates that the variability of crop yields is projected to increase in conjunction with increasing ΔGMT in many important regions for the four major staple crops. Such a hike an increase in yield volatility could have significant policy implications by affecting food prices and supplies, although management assumptions as well as model-structural limitations of the GGCMs to account for crop stress factors may impact the models' ability to project future changes in variability.

The scalability of each component (mean yields and yield variability) mean yields is conducive to the development of predictor functions relating ΔGMT, or other aggregate climate variables readily available from simplified climate models (such as pCO_2) to regional or global mean crop yield impacts. This lays the groundwork for a further exploration of the economic impacts of climate change encountered at target warming levels or over policy relevant regions.

Data availability. The coefficients estimated with Equations 1 to 3 are available as a Supplement, along with supplementary figures and RMSE estimates, at https://cloud.pik-potsdam.de/index.php/s/5J8vDoQvycH2nuZ https://doi.org/10.5281/zenodo.1194045 . The GGCM simulations that the analysis in this paper is based on are available through https://esg.pik-potsdam.de/search/isimip-ft/, with additional documentation available on the ISIMIP website https://www.isimip.org/outputdata/caveats-fast-track/

Acknowledgements. This work was supported within the framework of the Leibniz Competition (SAW-2013 PIK-5)and , by the EU FP7 HELIX project (grant no. 603864). , and by the German Federal Ministry for the Environment, Nature Conservation and Nuclear Safety (16_II_148_Global_A_IMPACT).

For their roles in producing, coordinating, and making available the ISIMIP model output, we acknowledge the modelling groups (listed in Table 1 of this paper) and the ISIMIP cross sectoral science team.

urlstyle

Blanc, É.: Statistical emulators of maize, rice, soybean and wheat yields from global gridded crop models, Agricultural and Forest Meteorology, 236, 145–161, , 2017.

Carter, T. R., Hulme, M., & Lal, M.: General Guidelines on the Use of Scenario Data for Climate Impact and Adaptation Assessment, 2007.

Challinor, A. J. and Wheeler, T. R.: Crop yield reduction in the tropics under climate change: Processes and uncertainties, Agricultural and Forest Meteorology, 148, 343 – 356, 2008.

Darwin, R. and Kennedy, D.: Economic effects of CO2 fertilization of crops: transforming changes in yield into changes in supply, Environmental Modeling &Assessment, 5, 157–168, 2000.

Eyshi Rezaei, E., Gaiser, T., S., S., B., S., and Ewert, F.: Combined impacts of climate and nutrient fertilization on yields of pearl millet in Niger, European Journal of Agronomy, 55, 77–88, 2014.

FAO: FertiSTAT - Fertilizer Use Statistics, Food and Agriculture Organization of the United Nations, Rome, 2007.

Frieler, K., Schauberger, B., Arneth, A., Balkovič, J., Chryssanthacopoulos, J., Deryng, D., Elliott, J., Folberth, C., Khabarov, N., Müller, C., Olin, S., Pugh, T. A. M., Schaphoff, S., Schewe, J., Schmid, E., Warszawski, L., and Levermann, A.: Understanding the weather signal in national crop-yield variability, Earth's Future, accepted.

Frieler, K., Levermann, A., Elliott, J., Heinke, J., Arneth, A., Bierkens, M. F. P., Ciais, P., Clark, D. B., Deryng, D., Döll, P., Falloon, P., Fekete, B., Folberth, C., Friend, A. D., Gellhorn, C., Gosling, S. N., Haddeland, I., Khabarov, N., Lomas, M., Masaki, Y., Nishina, K., Neumann, K., Oki, T., Pavlick, R., Ruane, A. C., Schmid, E., Schmitz, C., Stacke, T., Stehfest, E., Tang, Q., Wisser, D., Huber, V., Piontek, F., Warszawski, L., Schewe, J., Lotze-Campen, H., and Schellnhuber, H. J.: A framework for the cross-sectoral integration of multi-model impact projections: land use decisions under climate impacts uncertainties, Earth System Dynamics, 6, 447–460, , 2015.

Frieler, K., Meinshausen, M., Mengel, M., Braun, N., and Hare, W.: A Scaling Approach to Probabilistic Assessment of Regional Climate Change, Journal of Climate, 25, 3117–3144, 2012.

Gilbert, C. L. and Morgan, C. W.: Food price volatility, Philosophical Transactions of the Royal Society of London B: Biological Sciences, 365, 3023–3034, 2010.

Giorgi, F.: A Simple Equation for Regional Climate Change and Associated Uncertainty, Journal of Climate, 21, 1589–1604, 2008.

Heinke, J., Ostberg, S., Schaphoff, S., Frieler, K., Müller, C., Gerten, D., Meinshausen, M., and Lucht, W.: A new climate dataset for systematic assessments of climate change impacts as a function of global warming, Geoscientific Model Development, 6, 1689–1703, 2013.

Hempel, S., Frieler, K., Warszawski, L., Schewe, J., and Piontek, F.: A trend-preserving bias correction – the ISI-MIP approach, Earth System Dynamics, 4, 219–236, 2013.

IFA: Fertilizer Use by Crop, 5th edn, Rome, 2002.

Jaggard, K. W., Qi, A., and Ober, E. S.: Possible changes to arable crop yields by 2050, Philosophical Transactions of the Royal Society of London B: Biological Sciences, 365, 2835–2851, 2010.

Kimball, B. A.: Carbon Dioxide and Agricultural Yield: An Assemblage and Analysis of 430 Prior Observations1, Agronomy Journal, 75, 779, 1983.

Lindeskog, M., Arneth, A., Bondeau, A., Waha, K., Schurgers, G., Olin, S., and Smith, B.: Effects of crop phenology and management on the terrestrial carbon cycle: case study for Africa, Earth System Dynamics Discussions, 4, 235–278, 2013.

Lindeskog, M., Arneth, A., Bondeau, A., Waha, K., Seaquist, J., Olin, S., and Smith, B.: Implications of accounting for land use in simulations of ecosystem carbon cycling in Africa, Earth System Dynamics, 4, 385–407, , 2013.

Lobell, D. B., Sibley, A., and Ivan Ortiz-Monasterio, J.: Extreme heat effects on wheat senescence in India, Nature Climate Change, 2, 186–189, 2012.

Lotze-Campen, H., Müller, C., Bondeau, A., Rost, S., Popp, A., and Lucht, W.: Global food demand, productivity growth, and the scarcity of land and water resources: a spatially explicit mathematical programming approach, Agricultural Economics, 39, 325–338, , 2008.

Meinshausen, M., Smith, S. J., Calvin, K., Daniel, J. S., Kainuma, M. L. T., Lamarque, J.-F., Matsumoto, K., Montzka, S. A., Raper, S. C. B., Riahi, K., Thomson, A., Velders, G. J. M., and van Vuuren, D. P.: The RCP greenhouse gas concentrations and their extensions from 1765 to 2300, Climatic Change, 109, 213–241, 2011.

Mendelsohn, R., Basist, A., Dinar, A., Kurukulasuriya, P., and Williams, C.: What explains agricultural performance: climate normals or climate variance?, Climatic Change, 81, 85–99, 2007.

Mitchell, T. D.: Pattern scaling: an examination of the accuracy of the technique for describing future climates, Climatic Change, 60, 217–242, 2003.

Müller, C., Elliott, J., and Levermann, A.: Fertilizing hidden hunger, Nature Climate Change, 4, 540–541, Online: , 2014.

Müller, C. and Robertson, R. D.: Projecting future crop productivity for global economic modeling, Agricultural Economics, 45, 37–50, 2014.

Nelson, G. C., van der Mensbrugghe, D., Ahammad, H., Blanc, E., Calvin, K., Hasegawa, T., Havlik, P., Heyhoe, E., Kyle, P., Lotze-Campen, H., von Lampe, M., Mason d'Croz, D., van Meijl, H., Müller, C., Reilly, J., Robertson, R., Sands, R. D., Schmitz, C., Tabeau, A., Takahashi, K., Valin, H., and Willenbockel, D.: Agriculture and climate change in global scenarios: why don't the models agree, Agricultural Economics, 45, 85–101, 2014.

Ostberg, S., Lucht, W., Schaphoff, S., and Gerten, D.: Critical impacts of global warming on land ecosystems, Earth System Dynamics, 4, 347–357, 2013.

Parry, M., Rosenzweig, C., and Livermore, M.: Climate change, global food supply and risk of hunger, Philosophical Transactions of the Royal Society of London B: Biological Sciences, 360, 2125–2138, 2005.

Peng, S., Huang, J., Sheehy, J. E., Laza, R. C., Visperas, R. M., Zhong, X., Centeno, G. S., Khush, G. S., and Cassman, K. G.: Rice yields decline with higher night temperature from global warming, Proceedings of the National Academy of Sciences, 101, 9971–9975, 2004.

Portmann, F. T., Siebert, S., and Döll, P.: MIRCA2000-Global monthly irrigated and rainfed crop areas around the year 2000: A new high-resolution data set for agricultural and hydrological modeling, GlobalBiogeochemical Cycles, 24, 2010.

Ramankutty, N., Foley, J. A., Norman, J., and McSweeney, K.: The global distribution of cultivable lands: current patterns and sensitivity to possible climate change, Global Ecology and Biogeography, 11, 377–392, 2002.

Rosenzweig, C., Elliott, J., Deryng, D., Ruane, A. C., Müller, C., Arneth, A., Boote, K. J., Folberth, C., Glotter, M., Khabarov, N., Neumann, K., Piontek, F., Pugh, T. A. M., Schmid, E., Stehfest, E., Yang, H., and Jones, J. W.: Assessing agricultural risks of climate change in the 21st century in a global gridded crop model intercomparison, Proceedings of the National Academy of Sciences, 111, 3268–3273, Online: , 2014.

Santer, B. D., Wigley, T. M., Schlesinger, M. E., and Mitchell, J. F.: Developing climate scenarios from equilibrium GCM results, Max-Planck-Institut für Meteorologie Report, 47, 1990.

Schewe, J., Heinke, J., Gerten, D., Haddeland, I., Arnell, N. W., Clark, D. B., Dankers, R., Eisner, S., Fekete, B. M., Colón-González, F. J., Gosling, S. N., Kim, H., Liu, X., Masaki, Y., Portmann, F. T., Satoh, Y., Stacke, T., Tang, Q., Wada, Y., Wisser, D., Albrecht, T., Frieler, K., Piontek, F., Warszawski, L., and Kabat, P.: Multi-model assessment of water scarcity under climate change, Proceedings of the National Academy of Sciences, 111, 3245–3250, Online: , 2014.

Schlenker, W. and Roberts, M. J.: Nonlinear temperature effects indicate severe damages to U.S. crop yields under climate change, Proceedings of the National Academy of Sciences, 106, 15 594–15 598, 2009.

Smith, P., Gregory, P. J., van Vuuren, D., Obersteiner, M., Havlk, P., Rounsevell, M., Woods, J., Stehfest, E., and Bellarby, J.: Competition for land, Philosophical Transactions of the Royal Society of London B: Biological Sciences, 365, 2941–2957, 2010.

Solomon, S., Plattner, G.-K., Knutti, R., and Friedlingstein, P.: Irreversible climate change due to carbon dioxide emissions, Proceedings of the National Academy of Sciences, 106, 2009.

Stehfest, E., van Vuuren, D., Bouwman, L., and Kram, T.: Integrated assessment of global environmental change with IMAGE 3.0: Model description and policy applications, Netherlands Environmental Assessment Agency (PBL) , The Hague, 2014.

van der Velde, M., Tubiello, F. N., Vrieling, A., and Bourani, F. : Impacts of extreme weather on wheat and maize in France: Evaluating regional crop simulations against observed data, Climatic Change, 113, 751–765, 2012.

van Vuuren, D. P., Edmonds, J., Kainuma, M., Riahi, K., Thomson, A., Hibbard, K., Hurtt, G. C., Kram, T., Krey, V., Lamarque, J.-F., Masui, T., Meinshausen, M., Nakicenovic, N., Smith, S. J., and Rose, S. K.: The representative concentration pathways: an overview, Climatic Change, 109, 5–31, 2011.

Waha, K., van Bussel, L. G. J., Müller, C., and Bondeau, A.: Climate-driven simulation of global crop sowing dates, Global Ecology and Biogeography, 21, 247–259, 2012.

Wang, D., Heckathorn, S. A., Wang, X., and Phlipott, S. M.: A meta-analysis of plant physiological and growth responses to temperature and elevated CO2, Oecologia, 169, 1–13, 2012.

Warszawski, L., Frieler, K., Huber, V., Piontek, F., Serdeczny, O., and Schewe, J.: The Inter-Sectoral Impact Model Intercomparison Project (ISI–MIP): Project framework, Proceedings of the National Academy of Sciences, 111, 3228–3232, , 2014.

Yin, X.: Improving ecophysiological simulation models to predict the impact of elevated atmospheric CO2 concentration on crop productivity, Annals of Botany, 112, 465–75, 2013.

References

Blanc, É.: Statistical emulators of maize, rice, soybean and wheat yields from global gridded crop models, Agricultural and Forest Meteorology, 236, 145–161, https://doi.org/10.1016/j.agrformet.2016.12.022, 2017.

Bondeau, A., Smith, P. C., Zaehle, S., Schaphoff, S., Lucht, W., Cramer, W., Gerten, D., Lotze-Campen, H., Müller, C., Reichstein, M., and Smith, B.: Modelling the role of agriculture for the 20th century global terrestrial carbon balance, Global Change Biology, 13, 679–706, https://doi.org/10.1111/j.1365-2486.2006.01305.x, 2007.

Brown, M. E. and Kshirsagar, V.: Weather and international price shocks on food prices in the developing world, Global Environmental Change, 35, 31–40, https://doi.org/10.1016/j.gloenvcha.2015.08.003, 2015.

Challinor, A. J. and Wheeler, T. R.: Crop yield reduction in the tropics under climate change: Processes and uncertainties, Agricultural and Forest Meteorology, 148, 343 – 356, https://doi.org/10.1016/j.agrformet.2007.09.015, 2008.

Darwin, R. and Kennedy, D.: Economic effects of CO2 fertilization of crops: transforming changes in yield into changes in supply, Environmental Modeling & Assessment, 5, 157–168, https://doi.org/10.1023/A:1019013712133, 2000.

Deryng, D., Sacks, W. J., Barford, C. C., and Ramankutty, N.: Simulating the effects of climate and agricultural management practices on global crop yield, Global Biogeochemical Cycles, 25, GB2006, https://doi.org/10.1029/2009GB003765, gB2006, 2011.

Elliott, J., Kelly, D., Chryssanthacopoulos, J., Glotter, M., Jhunjhnuwala, K., Best, N., Wilde, M., and Foster, I.: The parallel system for integrating impact models and sectors (pSIMS), Environmental Modelling & Software, 62, 509–516, https://doi.org/10.1016/j.envsoft.2014.04.008, 2014.

Eyshi Rezaei, E., Gaiser, T., S., S., B., S., and Ewert, F.: Combined impacts of climate and nutrient fertilization on yields of pearl millet in Niger, European Journal of Agronomy, 55, 77–88, https://doi.org/10.1016/j.eja.2014.02.001, 2014.

FAO: FertiSTAT - Fertilizer Use Statistics, Food and Agriculture Organization of the United Nations, Rome, 2007.

Frieler, K., Meinshausen, M., Mengel, M., Braun, N., and Hare, W.: A Scaling Approach to Probabilistic Assessment of Regional Climate Change, Journal of Climate, 25, 3117–3144, https://doi.org/10.1175/JCLI-D-11-00199.1, 2012.

Frieler, K., Levermann, A., Elliott, J., Heinke, J., Arneth, A., Bierkens, M. F. P., Ciais, P., Clark, D. B., Deryng, D., Döll, P., Falloon, P., Fekete, B., Folberth, C., Friend, A. D., Gellhorn, C., Gosling, S. N., Haddeland, I., Khabarov, N., Lomas, M., Masaki, Y., Nishina, K., Neumann, K., Oki, T., Pavlick, R., Ruane, A. C., Schmid, E., Schmitz, C., Stacke, T., Stehfest, E., Tang, Q., Wisser, D., Huber, V., Piontek, F., Warszawski, L., Schewe, J., Lotze-Campen, H., and Schellnhuber, H. J.: A framework for the cross-sectoral integration of multi-model impact projections: land use decisions under climate impacts uncertainties, Earth System Dynamics, 6, 447–460, https://doi.org/10.5194/esd-6-447-2015, 2015.

Frieler, K., Schauberger, B., Arneth, A., Balkovič, J., Chryssanthacopoulos, J., Deryng, D., Elliott, J., Folberth, C., Khabarov, N., Müller, C., Olin, S., Pugh, T. A. M., Schaphoff, S., Schewe, J., Schmid, E., Warszawski, L., and Levermann, A.: Understanding the weather signal in national crop-yield variability, Earth's Future, 5, 605–616, https://doi.org/10.1002/2016EF000525, 2017.

Gilbert, C. L. and Morgan, C. W.: Food price volatility, Philosophical Transactions of the Royal Society of London B: Biological Sciences, 365, 3023–3034, https://doi.org/10.1098/rstb.2010.0139, 2010.

Giorgi, F.: A Simple Equation for Regional Climate Change and Associated Uncertainty, Journal of Climate, 21, 1589–1604, https://doi.org/10.1175/2007JCLI1763.1, 2008.

Golyandina, N. and Korobeynikov, A.: Basic Singular Spectrum Analysis and Forecasting with R, Computational Statistics and Data Analysis, 71, 934–954, R package version 0.14, 2014.

Golyandina, N., Korobeynikov, A., Shlemov, A., and Usevich, K.: Multivariate and 2D Extensions of Singular Spectrum Analysis with the Rssa Package, Journal of Statistical Software, 67, 1–78, https://doi.org/10.18637/jss.v067.i02, 2015.

Heinke, J., Ostberg, S., Schaphoff, S., Frieler, K., Müller, C., Gerten, D., Meinshausen, M., and Lucht, W.: A new climate dataset for systematic assessments of climate change impacts as a function of global warming, Geoscientific Model Development, 6, 1689–1703, https://doi.org/10.5194/gmd-6-1689-2013, 2013.

Hempel, S., Frieler, K., Warszawski, L., Schewe, J., and Piontek, F.: A trend-preserving bias correction – the ISI-MIP approach, Earth System Dynamics, 4, 219–236, https://doi.org/10.5194/esd-4-219-2013, 2013.

IFA: Fertilizer Use by Crop, 5th edn, International Fertilizer Industry Association (IFA), International Fertilizer Development Center (IFDC), International Potash Institute (IPI), Potash and Phosphate Institute (PPI), and Food and Agriculture Organization (FAO), Rome, 2002.

IPCC-TGICA: General Guidelines on the Use of Scenario Data for Climate Impact and Adaptation Assessment, Tech. rep., prepared by T.R. Carter on behalf of the Intergovernmental Panel on Climate Change, Task Group on Data and Scenario Support for Impact and Climate Assessment, 2007.

Jaggard, K. W., Qi, A., and Ober, E. S.: Possible changes to arable crop yields by 2050, Philosophical Transactions of the Royal Society of London B: Biological Sciences, 365, 2835–2851, https://doi.org/10.1098/rstb.2010.0153, 2010.

Jones, J., Hoogenboom, G., Porter, C., Boote, K., Batchelor, W., Hunt, L., Wilkens, P., Singh, U., Gijsman, A., and Ritchie, J.: The DSSAT cropping system model, European Journal of Agronomy, 18, 235–265, https://doi.org/10.1016/S1161-0301(02)00107-7, modelling Cropping Systems: Science, Software and Applications, 2003.

Kimball, B. A.: Carbon Dioxide and Agricultural Yield: An Assemblage and Analysis of 430 Prior Observations1, Agronomy Journal, 75, 779–788, https://doi.org/10.2134/agronj1983.00021962007500050014x, 1983.

Korobeynikov, A.: Computation- and space-efficient implementation of SSA, Statistics and Its Interface, 3, 357–368, R package version 0.14, 2010.

Lindeskog, M., Arneth, A., Bondeau, A., Waha, K., Seaquist, J., Olin, S., and Smith, B.: Implications of accounting for land use in simulations of ecosystem carbon cycling in Africa, Earth System Dynamics, 4, 385–407, https://doi.org/10.5194/esd-4-385-2013, 2013.

Liu, J.: A GIS-based tool for modelling large-scale crop-water relations, Environmental Modelling & Software, 24, 411–422, https://doi.org/10.1016/j.envsoft.2008.08.004, 2009.

Liu, J., Williams, J. R., Zehnder, A. J., and Yang, H.: GEPIC – modelling wheat yield and crop water productivity with high resolution on a global scale, Agricultural Systems, 94, 478–493, https://doi.org/10.1016/j.agsy.2006.11.019, 2007.

Lobell, D. B., Sibley, A., and Ivan Ortiz-Monasterio, J.: Extreme heat effects on wheat senescence in India, Nature Climate Change, 2, 186–189, https://doi.org/10.1038/nclimate1356, 2012.

Lotze-Campen, H., Müller, C., Bondeau, A., Rost, S., Popp, A., and Lucht, W.: Global food demand, productivity growth, and the scarcity of land and water resources: a spatially explicit mathematical programming approach, Agricultural Economics, 39, 325–338, https://doi.org/10.1111/j.1574-0862.2008.00336.x, 2008.

McSweeney, C. F. and Jones, R. G.: How representative is the spread of climate projections from the 5 CMIP5 GCMs used in ISI-MIP?, Climate Services, 1, 24–29, https://doi.org/https://doi.org/10.1016/j.cliser.2016.02.001, 2016.

Meinshausen, M., Smith, S. J., Calvin, K., Daniel, J. S., Kainuma, M. L. T., Lamarque, J.-F., Matsumoto, K., Montzka, S. A., Raper, S. C. B., Riahi, K., Thomson, A., Velders, G. J. M., and van Vuuren, D. P.: The RCP greenhouse gas concentrations and their extensions from 1765 to 2300, Climatic Change, 109, 213–241, https://doi.org/10.1007/s10584-011-0156-z, 2011.

Mendelsohn, R., Basist, A., Dinar, A., Kurukulasuriya, P., and Williams, C.: What explains agricultural performance: climate normals or climate variance?, Climatic Change, 81, 85–99, https://doi.org/10.1007/s10584-006-9186-3, 2007.

Mitchell, T. D.: Pattern scaling: an examination of the accuracy of the technique for describing future climates, Climatic Change, 60, 217–242, https://doi.org/10.1023/A:1026035305597, 2003.

Müller, C. and Robertson, R. D.: Projecting future crop productivity for global economic modeling, Agricultural Economics, 45, 37–50, https://doi.org/10.1111/agec.12088, 2014.

Müller, C., Elliott, J., and Levermann, A.: Fertilizing hidden hunger, Nature Climate Change, 4, 540–541, https://doi.org/10.1038/nclimate2290, 2014.

Nelson, G. C., van der Mensbrugghe, D., Ahammad, H., Blanc, E., Calvin, K., Hasegawa, T., Havlik, P., Heyhoe, E., Kyle, P., Lotze-Campen, H., von Lampe, M., Mason d'Croz, D., van Meijl, H., Müller, C., Reilly, J., Robertson, R., Sands, R. D., Schmitz, C., Tabeau, A., Takahashi, K., Valin, H., and Willenbockel, D.: Agriculture and climate change in global scenarios: why don't the models agree, Agricultural Economics, 45, 85–101, https://doi.org/10.1111/agec.12091, 2014.

Ostberg, S., Lucht, W., Schaphoff, S., and Gerten, D.: Critical impacts of global warming on land ecosystems, Earth System Dynamics, 4, 347–357, https://doi.org/10.5194/esd-4-347-2013, 2013.

Oyebamiji, O. K., Edwards, N. R., Holden, P. B., Garthwaite, P. H., Schaphoff, S., and Gerten, D.: Emulating global climate change impacts on crop yields, Statistical Modelling, 15, 499–525, https://doi.org/10.1177/1471082X14568248, 2015.

Parry, M., Rosenzweig, C., and Livermore, M.: Climate change, global food supply and risk of hunger, Philosophical Transactions of the Royal Society of London B: Biological Sciences, 360, 2125–2138, https://doi.org/10.1098/rstb.2005.1751, 2005.

Peng, S., Huang, J., Sheehy, J. E., Laza, R. C., Visperas, R. M., Zhong, X., Centeno, G. S., Khush, G. S., and Cassman, K. G.: Rice yields decline with higher night temperature from global warming, Proceedings of the National Academy of Sciences, 101, 9971–9975, https://doi.org/10.1073/pnas.0403720101, 2004.

Portmann, F. T., Siebert, S., and Döll, P.: MIRCA2000-Global monthly irrigated and rainfed crop areas around the year 2000: A new high-resolution data set for agricultural and hydrological modeling, Global Biogeochemical Cycles, 24, GB1011, https://doi.org/10.1029/2008GB003435, 2010.

Ramankutty, N., Foley, J. A., Norman, J., and McSweeney, K.: The global distribution of cultivable lands: current patterns and sensitivity to possible climate change, Global Ecology and Biogeography, 11, 377–392, https://doi.org/10.1046/j.1466-822x.2002.00294.x, 2002.

Rosenzweig, C., Elliott, J., Deryng, D., Ruane, A. C., Müller, C., Arneth, A., Boote, K. J., Folberth, C., Glotter, M., Khabarov, N., Neumann, K., Piontek, F., Pugh, T. A. M., Schmid, E., Stehfest, E., Yang, H., and Jones, J. W.: Assessing agricultural risks of climate change in the 21st century in a global gridded crop model intercomparison, Proceedings of the National Academy of Sciences, 111, 3268–3273, https://doi.org/10.1073/pnas.1222463110, 2014.

Santer, B. D., Wigley, T. M., Schlesinger, M. E., and Mitchell, J. F.: Developing climate scenarios from equilibrium GCM results, Max-Planck-Institut für Meteorologie Report, 47, 1990.

Schewe, J., Heinke, J., Gerten, D., Haddeland, I., Arnell, N. W., Clark, D. B., Dankers, R., Eisner, S., Fekete, B. M., Colón-González, F. J., Gosling, S. N., Kim, H., Liu, X., Masaki, Y., Portmann, F. T., Satoh, Y., Stacke, T., Tang, Q., Wada, Y., Wisser, D., Albrecht, T., Frieler, K., Piontek, F., Warszawski, L., and Kabat, P.: Multimodel assessment of water scarcity under climate

change, Proceedings of the National Academy of Sciences, 111, 3245–3250, https://doi.org/10.1073/pnas.1222460110, 2014.

Schlenker, W. and Roberts, M. J.: Nonlinear temperature effects indicate severe damages to U.S. crop yields under climate change, Proceedings of the National Academy of Sciences, 106, 15 594–15 598, https://doi.org/10.1073/pnas.0906865106, 2009.

Smith, P., Gregory, P. J., van Vuuren, D., Obersteiner, M., Havlík, P., Rounsevell, M., Woods, J., Stehfest, E., and Bellarby, J.: Competition for land, Philosophical Transactions of the Royal Society of London B: Biological Sciences, 365, 2941–2957, https://doi.org/10.1098/rstb.2010.0127, 2010.

Solomon, S., Plattner, G.-K., Knutti, R., and Friedlingstein, P.: Irreversible climate change due to carbon dioxide emissions, Proceedings of the National Academy of Sciences, 106, https://doi.org/10.1073/pnas.0812721106, 2009.

Stehfest, E., van Vuuren, D., Bouwman, L., and Kram, T.: Integrated assessment of global environmental change with IMAGE 3.0: Model description and policy applications, Netherlands Environmental Assessment Agency (PBL), The Hague, 2014.

Tadesse, G., Algieri, B., Kalkuhl, M., and von Braun, J.: Drivers and triggers of international food price spikes and volatility, Food Policy, 47, 117–128, https://doi.org/10.1016/j.foodpol.2013.08.014, 2014.

Taylor, K. E., Stouffer, R. J., and Meehl, G. a.: An overview of CMIP5 and the experiment design, Bulletin of the American Meteorological Society, 93, 485–498, https://doi.org/10.1175/BAMS-D-11-00094.1, 2012.

van der Velde, M., Tubiello, F. N., Vrieling, A., and Bouraoui, F.: Impacts of extreme weather on wheat and maize in France: evaluating regional crop simulations against observed data, Climatic Change, 113, 751–765, https://doi.org/10.1007/s10584-011-0368-2, 2012.

van Vuuren, D. P., Edmonds, J., Kainuma, M., Riahi, K., Thomson, A., Hibbard, K., Hurtt, G. C., Kram, T., Krey, V., Lamarque, J.-F., Masui, T., Meinshausen, M., Nakicenovic, N., Smith, S. J., and Rose, S. K.: The representative concentration pathways: an overview, Climatic Change, 109, 5–31, https://doi.org/10.1007/s10584-011-0148-z, 2011.

Waha, K., van Bussel, L. G. J., Müller, C., and Bondeau, A.: Climate-driven simulation of global crop sowing dates, Global Ecology and Biogeography, 21, 247–259, https://doi.org/10.1111/j.1466-8238.2011.00678.x, 2012.

Warszawski, L., Frieler, K., Huber, V., Piontek, F., Serdeczny, O., and Schewe, J.: The Inter-Sectoral Impact Model Intercomparison Project (ISI–MIP): Project framework, Proceedings of the National Academy of Sciences, 111, 3228–3232, https://doi.org/10.1073/pnas.1312330110, 2014.